Dalton Transactions

RSC Publishing

PAPER

View Article Online
View Journal | View Issue

Cite this: *Dalton Trans.*, 2013, **42**, 11163

Synthesis, structural characterization and *cis–trans* isomerization of novel (salicylaldiminato)platinum(II) complexes†

Feng Zheng,[a,b] Alan T. Hutton,[a] Cornelia G. C. E. van Sittert,[c] John R. Moss‡[a] and Selwyn F. Mapolie*[b]

Received 16th May 2013,
Accepted 13th June 2013

DOI: 10.1039/c3dt51283e

www.rsc.org/dalton

The reaction of *cis*-[$PtCl_2$(dmso)] with the salicylaldimine ligand, *N*-(2-hydroxybenzylidene)-2,6-di-isopropylaniline, $\mathbf{L_A}$ in the presence of sodium acetate in methanol produced both *cis*- and *trans*-[$PtClL_A$(dmso)], **1a** and **1b**. An analogous reaction for the less bulky ligand, *N*-(2-hydroxybenzylidene)aniline $\mathbf{L_B}$ produced only *cis*-[$PtClL_B$(dmso)], **2**. The reactions of these dmso complexes with triphenylphosphine also yielded complexes with different geometries depending on the nature of the salicylaldiminato ligand. Thus the *cis–trans* isomerization of *cis*-[$PtClL_A(PPh_3)$] **3a** was investigated both experimentally and computationally, and a tetrahedral transition state was detected in this process. A good agreement of the experimental activation parameters with those determined theoretically using DFT was obtained. $\mathbf{L_A}$ was also reacted with [PtClMe(cod)] in methanol to yield the corresponding salicylaldiminato complex **6** in which the methyl group is *cis* to the imine nitrogen. X-ray crystal structures of some compounds obtained are reported.

Introduction

In the development of coordination chemistry, metal complexes with Schiff bases as ligands have played an important role, and have found extensive applications in a range of different fields. Schiff bases derived from salicylaldehydes and diamines have, for example, great potential applications in asymmetric catalysis.[1] Among other applications, salicylaldiminato ligands have been used in transition-metal complexes which have been employed as olefin transformation catalysts.[2,3] Moreover, they have also been found to have useful biological applications[4] and have been used as functional materials.[5] This has given great impetus to develop a variety of interesting salicylaldiminato-based metal complexes for applications in many other fields.

In transition metal-catalyzed olefin polymerization/oligomerization reactions, salicylaldiminato ligands, known as "Grubbs ligands", have been found to afford highly active catalysts for group 4,[6] group 6,[7] and group 10[2] metal systems. It has been demonstrated *via* computational studies that the reaction mechanism of the chain propagation step in olefin oligomerization/polymerization using salicylaldiminato catalysts is quite complex due to the potential presence of geometrical isomers, *i.e.*, the "initiator complexes" for chain propagation can have two different configurations dependent upon whether the alkyl group is *trans* to N or *trans* to O (Fig. 1).[8] Higher energies were obtained for isomers with the alkyl group *trans* to the more strongly donating nitrogen atom.[9] To the best of our knowledge, the *cis–trans*

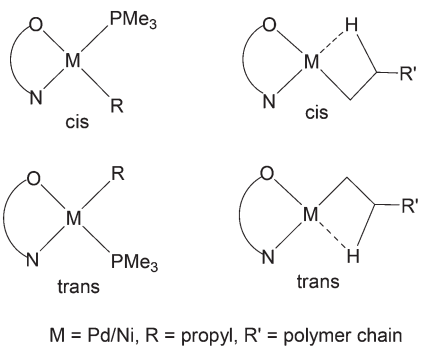

Fig. 1 Model for "initiator complexes" and intermediates with *cis* and *trans* geometries for the mechanism of the chain propagation step in ethylene oligomerization/polymerization catalyzed by salicylaldiminato (Grubbs) catalysts.[8]

[a]*Department of Chemistry, University of Cape Town, Private Bag, Rondebosch, 7700, South Africa*
[b]*Department of Chemistry and Polymer Science, Stellenbosch University, Private Bag, Matieland, 7601, Stellenbosch, South Africa. E-mail: smapolie@sun.ac.za*
[c]*Catalysis and Synthesis Research Group, Chemical Resource Beneficiation Focus Area, North-West University, Potchefstroom, 2520, South Africa*

†Electronic supplementary information (ESI) available. CCDC 931185–931189. For ESI and crystallographic data in CIF or other electronic format see DOI: 10.1039/c3dt51283e

‡John Moss is deceased.

isomerization of salicylaldiminato metal complexes has not been reported experimentally.

Salicylaldiminato platinum(II) complexes have also been recently found to exhibit pronounced phosphorescent properties.[5] For example, ultrasound-induced phosphorescent emission were reported to be observed with chiral, clothespin-shaped *trans*-bis(salicylaldiminato)Pt(II) complexes.[5a] However, the use of this class of platinum complexes is very rare in catalysis, probably due to their generally high kinetic and thermodynamic stability. On the other hand, the enhanced stability of platinum(II) complexes relative to their palladium analogues makes them easier to handle and thus easier to study their chemistry. The series of salicylaldiminato Pt(II) compounds reported here can be potential model complexes for their Pd analogues which have shown catalytic activity for the transformation of unsaturated hydrocarbons.[10] Furthermore, these complexes could potentially be biological active as some of their Pd analogues have shown antitumor activities.[4a,b]

We are interested in developing the chemistry of (salicylaldiminato)platinum(II) complexes before pursuing further work with possible applications, in particular investigating the coordination chemistry of the salicylaldiminato ligands. The present study is focused on three issues: (1) an evaluation of the steric effect on coordination behaviour of two salicylaldiminato (N^O) ligands in the synthesis of platinum(II) complexes, (2) a comparative analysis of the reactivity and structure of the Pt(N^O) complexes, and (3) a combined experimental and theoretical investigation of the *cis–trans* isomerization of a Pt(N^O) complex.

Results and discussion

Synthesis of dmso-ligated (salicylaldiminato)platinum(II) complexes

The reaction of the salicylaldiminato ligand $\mathbf{L_A}$ with *cis*-$[PtCl_2(dmso)_2]$ in the presence of sodium acetate in a 1 : 1 : 1 mole ratio was carried out in refluxing methanol for 16 h. Two geometrical isomers, in which the dmso group is either *cis* to N (*cis* isomer, **1a**) or *trans* to N (*trans* isomer, **1b**), were obtained [Scheme 1(A)]. The use of column chromatography allowed the separation of these two isomers.

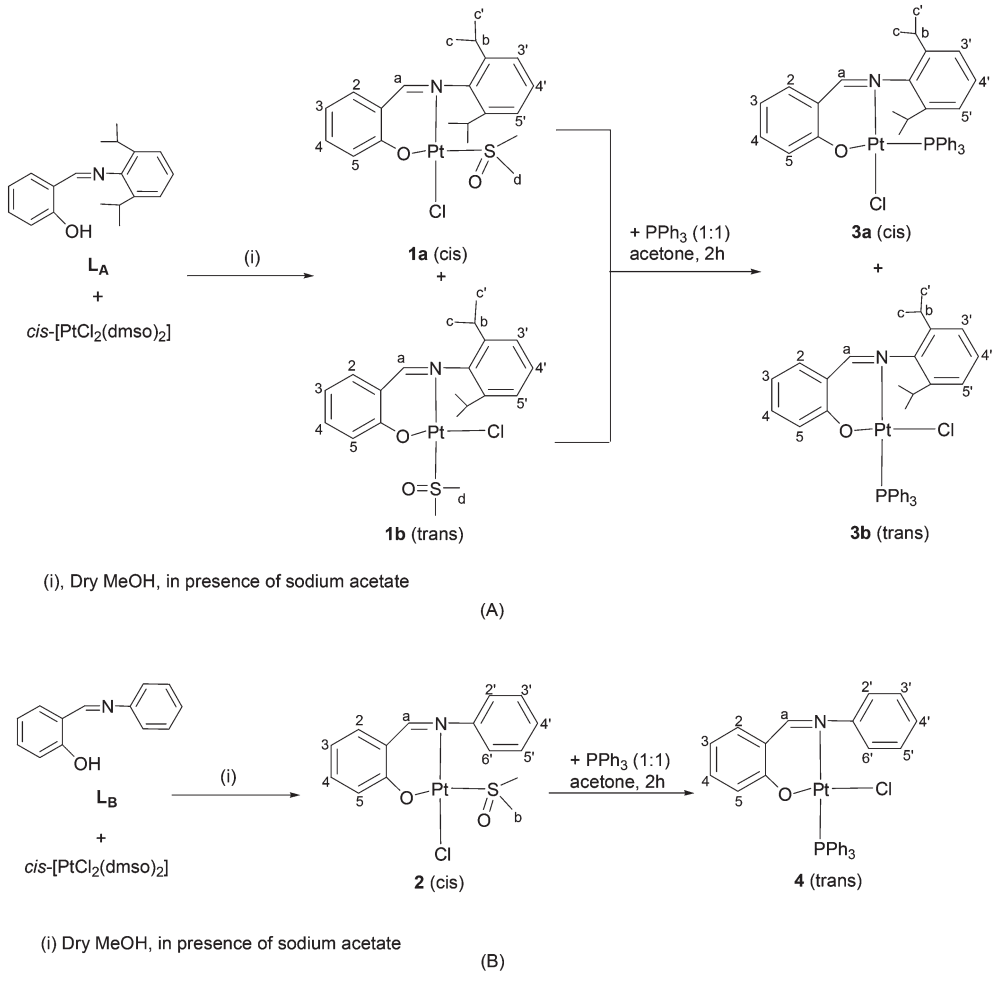

Scheme 1 Preparation of salicylaldiminato platinum(II) complexes, where *cis* means L (dmso or PPh_3) *cis* to N, while *trans* means L *trans* to N.

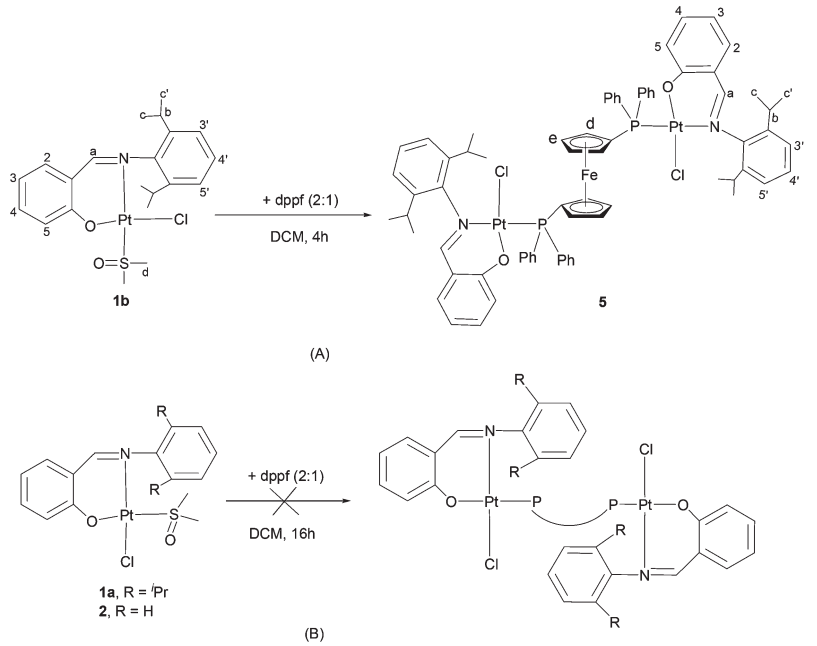

Scheme 2 Reactions of dppf with dmso-ligated complexes **1–2**.

Different reaction conditions were employed to investigate potential changes in the isomer ratio. When the reaction was carried out at room temperature or under reflux for a short time (30 min), the isolated product contained mainly the *cis* isomer, but longer reflux times gave more of the *trans* isomer (see Table S1 in ESI†). These observations suggested that the *cis* isomer **1a** is the kinetically favoured product.

In order to determine any steric effects of the ligand, platinum complex **2** was synthesized by the reaction of the less bulky ligand, $\mathbf{L_B}$, with *cis*-$[PtCl_2(dmso)_2]$ under the same reaction conditions. In this case, complex **2** precipitated out of the solution as a single geometric isomer, in which the dmso group is *cis* to the N atom of the chelating ligand [Scheme 1(B)].

The reactions of the monodentate phosphine, PPh_3 with dmso complexes **1a**, **1b** and **2** were studied and the resulting products are depicted in Scheme 1. When the dmso complexes **1a** or **1b** were reacted with PPh_3 in a 1 : 1 mole ratio in acetone at room temperature, two isomers **3a** and **3b**, with the PPh_3 ligand in a *cis* or *trans* position to the nitrogen atom, were isolated [Scheme 1(A)]. A different behaviour was observed in the case of complex **2** which contains the less sterically bulky N^O ligand, as its reaction with PPh_3 (1 : 1) in acetone only gave product **4** with a *trans* arrangement of the PPh_3 and the nitrogen atom [Scheme 1(B)]. This is despite the fact that the precursor is in the *cis* form.

Reactions of **1a**, **1b** and **2** with diphosphines (in a 2 : 1 ratio) proved more difficult. The success of the ligand displacement depends on the nature of diphosphines, and the geometry of the dmso–platinum complex. For dppe, no target products were obtained from reactions with either complexes **1–2**. When a diphosphine with a much longer skeletal backbone, such as dppf, was used, the desired dimeric complex, **5**, was formed from the *trans* complex **1b**. In complex **5** two individual organoplatinum(II) units are combined in one molecular system *via* a dppf spacer. However, no product is formed from the reactions of dppf with the *cis* complexes **1a** and **2** due to the steric hindrance (Scheme 2).

The dmso-ligated platinum(II) complexes **1–2** and their PPh_3 derivatives **3–4** were obtained as bright yellow crystalline solids after recrystallization from CH_2Cl_2–MeOH or CH_2Cl_2–*n*-hexane, while the diplatinum(II) complex with a dppf spacer, **5**, was isolated as an orange powder. All the triphenylphosphine complexes were found to be highly thermally as well as air stable in the solid state. The identity of these (salicylaldiminato)platinum(II) complexes was confirmed by elemental analysis (C, H, N), mass spectrometry, IR and NMR (^{1}H, 2D-COSY, 2D-HSQC, ^{13}C and ^{31}P) spectroscopies. The solid state structures of two pairs of isomers, **1a**/**1b** and **3a**/**3b**, and **2** were determined by X-ray crystallography.

Spectroscopic properties of complexes

IR spectra. The most informative peak in the IR spectra, the ν(C=N) stretch, appears at 1624 and 1613 cm^{-1} for the salicylaldimine ligands $\mathbf{L_A}$ and $\mathbf{L_B}$, respectively. This is a red-shift relative to the ligand in all the platinum(II) complexes as shown in Table 1. The red-shift indicates the coordination of the imine nitrogen to the platinum centre resulting in a weakening of the bond between C and N.[11] Furthermore, the disappearance of the band at 2884 cm^{-1} (due to the OH) confirmed the deprotonation of the hydroxyl group and formation of a σ-bond between O and the metal centre.

A strong peak at *ca.* 1155 cm^{-1}, assigned to the ν(S=O) stretch, is observed in the IR spectra of the *cis* dmso complexes **1a** and **2**, while this peak for *trans* **1b** appears at lower wavenumber, around 1140 cm^{-1}. This indicates that the bond between S and O of the *cis* complex is stronger than that of the

Table 1 Selected spectroscopic data (IR, MS, ^{1}H, and ^{13}C NMR) for (salicylaldiminato)platinum(II) complexes **1–6**

	IR/cm^{-1}		^{1}H NMR				^{13}C NMR			^{31}P NMR
Complex	$\nu_{S=O}$	$\nu_{C=N}$	H^a	H^b	H^d	H^5	C^a	C^d	C^5	
1a[a]	1154	1606	7.81 (s, J_{Pt-H} = 93.3 Hz)	3.59	3.40[b] (s, J_{Pt-H} = 18.7 Hz)	6.71 (td, 7.33, 1.06 Hz)	163.2	47.3[b]	117.3	
1b	1140	1606	7.81 (s, J_{Pt-H} = 63.3 Hz)	3.36	3.39[b] (s, J_{Pt-H} = 13.9 Hz)	6.73 (td, 7.83 Hz)	161.3	42.3[b]	117.3	
2[a]	1155	1607	7.83 (s, J_{Pt-H} = 86.3 Hz)		3.24[b] (s, J_{Pt-H} = 16.5 Hz)	6.64 (d, 7.42 Hz)	162.7	46.4[b]	117.6	−2.14 (J_{Pt-P} = 4064 Hz)
3a[a]		1607	7.61 (s)	3.66		7.19 (d, 8.76 Hz)	163.94		122.05	8.87 (J_{Pt-P} = 3819 Hz)
3b		1610	8.06 (d, J_{P-H} = 13.9 Hz)	3.53		6.31 (dd, 8.57, 0.49 Hz)	160.48		121.10	7.40 (J_{Pt-P} = 3869 Hz)
4[a]		1608	8.20 (d, J_{P-H} = 13.4 Hz)			6.16 (d, 8.62 Hz)	160.89		121.86	1.98 (J_{Pt-P} = 3851 Hz)
5		1610	8.03 (d, J_{P-H} = 9.5 Hz)	3.50		6.14 (d, 8.60 Hz)	160.68		120.98	20.43 (J_{Pt-P} = 4400 Hz)
6		1608	8.11 (d, J_{P-H} = 12.2 Hz, J_{Pt-H} = 70.9 Hz)		−0.29[c] (d, J_{P-H} = 3.2 Hz, J_{Pt-H} = 73.3 Hz)	6.48–6.42 (m)	162.12 (s)	−18.93[c] (d, J_{P-C} = 8.97 Hz)		

[a] L is *cis* to N atom (L = dmso, PPh_3). [b] H^{dmso}/C^{dmso}. [c] H^{Me}/C^{dmso}.

trans species. The displacement of the dmso group by phosphines in complexes **3–5** was confirmed by the disappearance of the ν(S=O) band and the appearance of strong absorption bands at 1434 cm^{-1} due to the C–P bond.

NMR spectra. In the ^{1}H NMR spectra of dmso complexes **1a**, **1b** and **2**, the disappearance of the phenolic proton around δ 13.5 ppm and the observation of the upfield shift of the imine proton (H^a) at *ca.* 7.8 ppm (see Table 1) relative to that of the free ligands, suggests successful deprotonation and formation of a phenoxy σ-bond with the metal centre, consistent with the IR data for the complexes. For the *cis* complexes **1a** and **2**, the imine protons display large J_{Pt-H} values of 93.3 and 86.3 Hz, respectively, consistent with the presence of a chloride ligand in a *trans* position to the nitrogen atom. Conversely, for the *trans* complex **1b**, the J_{Pt-H} for the imine hydrogen is reduced (63.3 Hz) compared to the *cis* isomer as shown in Fig. 2, which is consistent with the presence of a dimethylsulfoxide ligand in a position *trans* to the nitrogen atom. A similar phenomenon has been observed for other platinum coordination compounds.[12] The signal of the dmso methyl protons for the *trans* complex **1b** appears at lower field compared to that of the *cis* complex **1a**.

By replacing the dmso group with PPh_3, all the imine protons (H^a) of the complexes with *trans* geometry (where PPh_3 is *trans* to the imine), **3b** and **4**, were observed in the region 8.03–8.20 ppm. These observations indicate that π back-bonding from platinum into empty low lying p-based orbitals is more pronounced compared to s-based orbitals and leads to the slight elongation of the Pt–N bonds in the complexes. This consequently results in a downfield shift of 0.08–0.37 ppm with respect to their dmso precursors. In the case of the *trans* complexes with phosphine ligands, **3b**, **4** and **5**, the imine proton appears as doublets with $^4J_{(PH)}$ of 13.4–13.9 Hz, while in the ^{1}H NMR spectrum of the *cis* complex **3a** the chemical shift of the imine proton shifted to higher field and appeared as a singlet (see Fig. 3). However, no coupling of the imine proton with the ^{195}Pt nuclei was observed in all cases. Similar observations have been previously reported in the literature for related platinum complexes.[13]

For the *trans* phosphine-containing complexes **3b**, **4** and **5**, another salient feature observed in the ^{1}H NMR spectra was the chemical shift of the aromatic proton H^5, which moved up-field to the region 6.14–6.31 ppm compared to their dmso precursors as shown in Table 1. This has been ascribed to the anisotropic shielding effect of the aromatic ring current that a phenyl group in PPh_3 has on the H^5 proton pointing towards it.[14]

For all (salicylaldiminato)platinum(II) complexes containing $\mathbf{L_A}$ except **3a** (see Fig. 3), signals corresponding to the methyl protons of the isopropyl moieties ($H^{c/c'}$) on the ligands were split into two doublets, indicating that rotations between the nitrogen and the *ipso* carbon of these complexes are restricted.

The ^{31}P NMR spectra show singlets for the phosphine-containing platinum(II) complexes, **3–5**, with resolved coupling to ^{195}Pt. With the bulky ligand $\mathbf{L_A}$, the *cis* isomer **3a** shows an even higher-field shift ($\Delta\delta$ = −2.14 ppm) compared to its *trans*

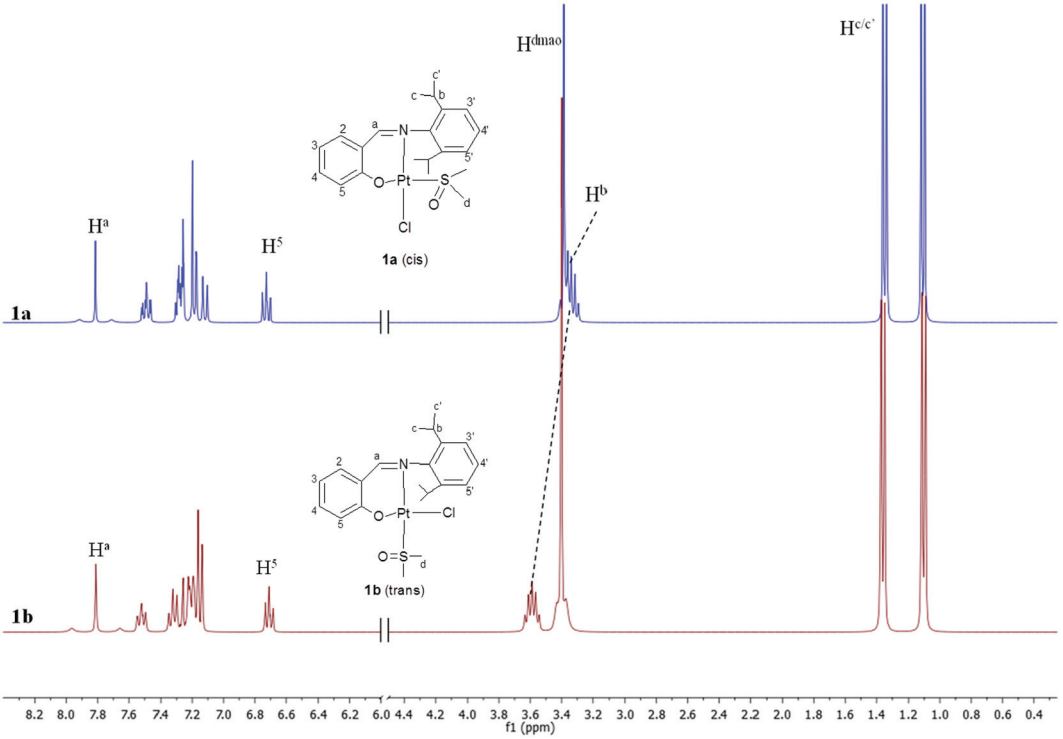

Fig. 2 A comparison of the ^{1}H NMR spectra of *cis*- and *trans*-[PtClL_A(dmso)], **1a** and **1b**.

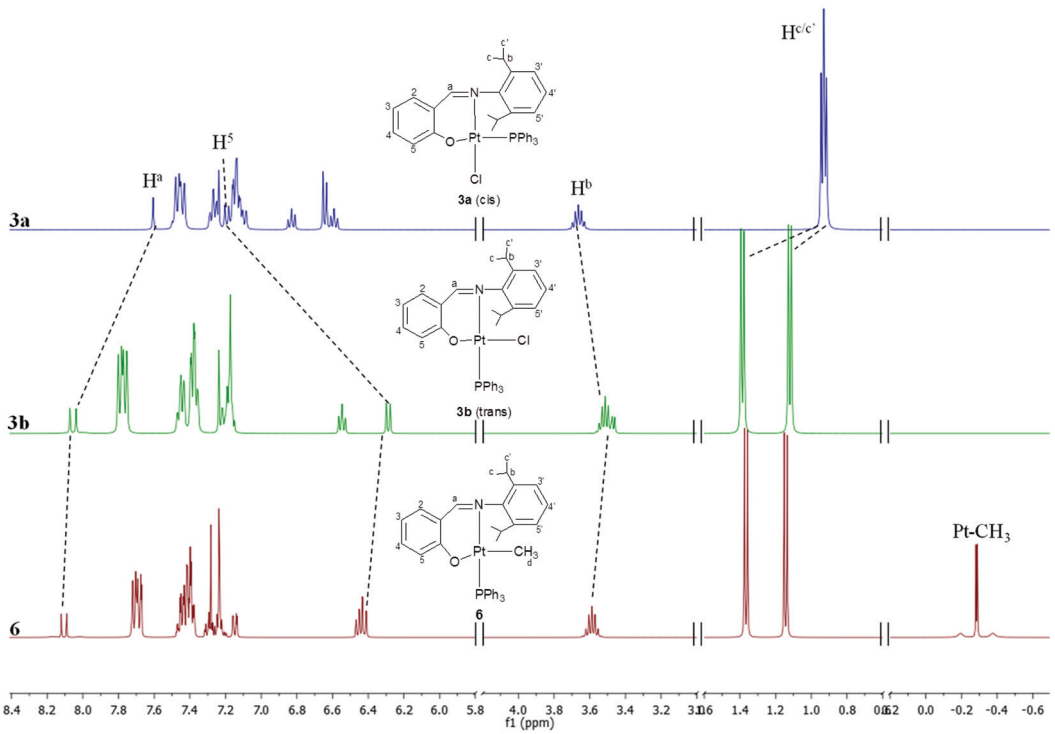

Fig. 3 A comparison of the ^{1}H NMR spectra of *cis*- and *trans*-[PtClL_A(PPh_3)], **3a** and **3b**, as well as the methyl analogue **6**.

isomer **3b** ($\Delta\delta$ = 8.87 ppm), suggesting that the *cis* arrangement of the oxygen atom and the imine nitrogen enhances the shielding effect. In addition, the chemical shift of the P atoms in **5** appeared at higher field ($\Delta\delta$ = 1.98 ppm) compared to the PPh_3-containing mononuclear analogue **3b**, due to the electron rich ferrocenyl moiety of the spacer ligand.

The $^{1}J_{Pt-P}$ coupling constants were measured as 4062 Hz in *cis* complex **3a** and *ca.* 3850 Hz in *trans* complexes **3b**, **4** and **5** (see Table 1), which are of the order of magnitude expected for a P atom *trans* to an O atom.[13,15,16] The magnitude of $^{1}J_{Pt-P}$ coupling constants is a measure of the strength of the Pt–P σ bonding.[17] Thus the lower values for the *trans* complexes are indicative of a weakening of the Pt–P σ bonding compared to those of the *cis* complex, **3a**. Interestingly, there is a *ca.* 6% increase in the $^{1}J_{Pt-P}$ for the *cis* isomer **3a** over its *trans* isomer **3b**, probably due to a higher *trans* influence of the imine nitrogen compared to that of the coordinated oxygen, which as a consequence weakens the Pt–P σ bond in **3b**.

In the ^{13}C NMR spectrum, coordination of the imine nitrogen was confirmed by the downfield shifts of the imine carbon signal (C^{a}) with respect to the free ligands. The signal for the imine carbon of the *cis* complex **1a** appears more upfield than that for the *trans* isomer **1b**. The signal for the methyl carbons of dmso (C^{dmso}) occurs as a doublet at approximately 47 ppm for all dmso-ligated complexes except **1b**. The peak of C^{dmso} in **1b** appears more upfield (42.31 ppm) than its *cis* isomer **1a**. No significant shifts in ^{13}C resonances were observed for the phosphine complexes compared to their dmso precursors. The differences between the *cis*/*trans* isomers **3a** and **3b** in their ^{13}C spectra are consistent with the trends observed for their dmso precursors.

Crystallographic studies

X-ray quality crystals of some of the complexes were obtained by cooling a concentrated solution of the complex in dichloromethane-methanol to 4 °C. The molecular structures of dmso-ligated complexes **1a**, **1b** and **2**, and the PPh_3 derivatives **3a**, and **3b** were determined by single crystal X-ray structural analysis. The structure of **1b** consists of discrete monomeric molecules with two different geometries [**1b**(A) and **1b**(B)]. These conformations are not significantly different in terms of structural parameters such as bond lengths or angles. This phenomenon is common place in the literature for related platinum and palladium complexes.[12,16,18] The ORTEP plots of **1–3** are shown in Fig. 4–8.

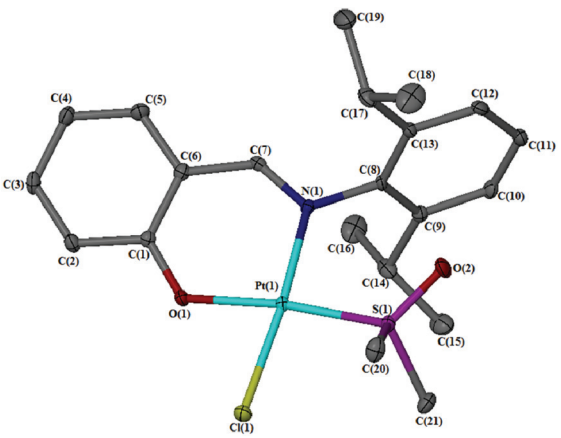

Fig. 4 ORTEP view of **1a**. Ellipsoids are drawn at the 30% probability level.

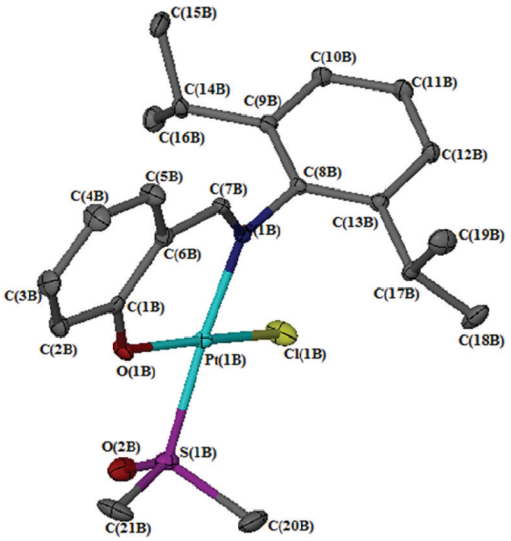

Fig. 5 ORTEP view of molecule B in **1b**. Ellipsoids are drawn at the 30% probability level.

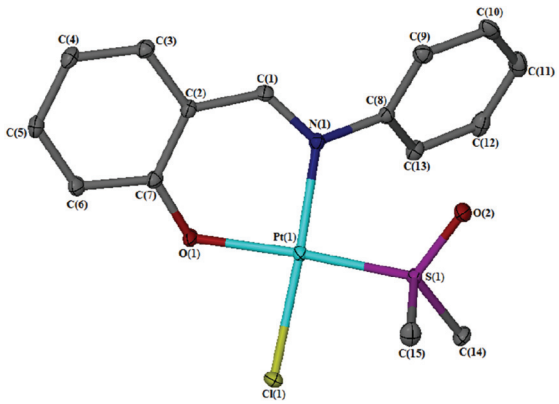

Fig. 6 ORTEP view of **2**. Ellipsoids are drawn at the 30% probability level.

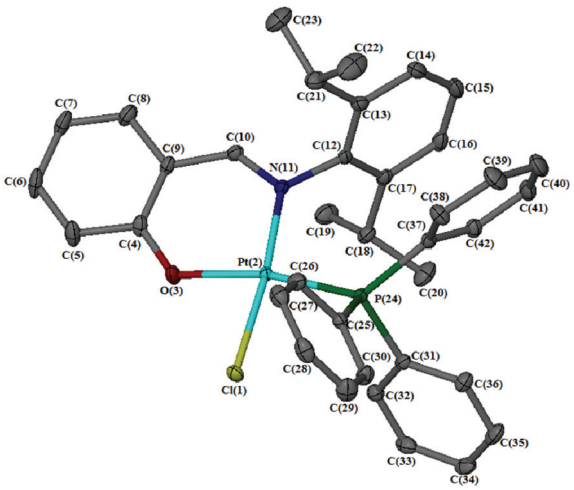

Fig. 7 ORTEP view of **3a**. Ellipsoids are drawn at the 40% probability level.

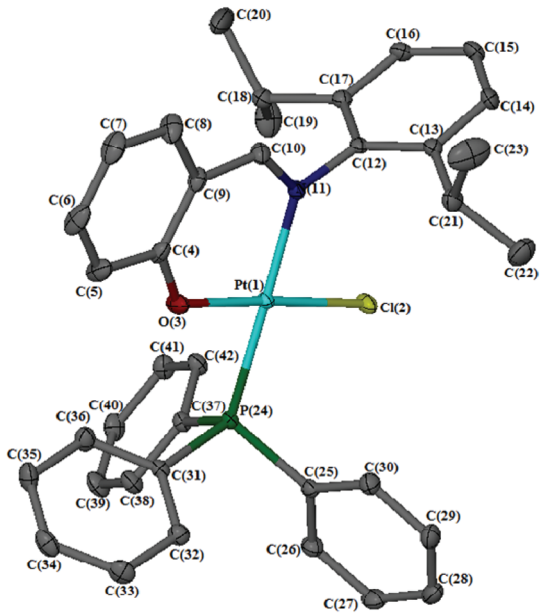

Fig. 8 ORTEP view of **3b**. Ellipsoids are drawn at the 40% probability level.

Relevant crystal data for all structures are given in Table 2 along with selected bond lengths and angles in Table 3.

For all complexes, the coordination sphere of platinum is square-planar with the κ^2-N^O-bound bidentate ligands, the chlorido ligand and the S-bound dimethylsulfoxide (**1a**, **1b** and **2**), or P-bound triphenylphosphine (**3a** and **3b**) completing the coordination sphere. The molecular structures provide decisive evidence of the fact that in **1b** and **3b** the dmso or PPh_3 ligand occupies the position *trans* to the imine nitrogen, while in **1a**, **2** and **3a** it occupies the *cis* position. These complexes have fused bicyclic systems containing a six-membered metal-containing ring and the phenyl group. As shown in Table 3, bond lengths and angles are well within the range of values obtained for analogous compounds.[19]

In all cases, the angles between adjacent atoms in the coordination sphere are close to the expected value of 90°, and the sum of the angles around platinum is around 360°. The most noticeable distortion occurs in the O–Pt–Cl angle in the *cis* complexes **1a** and **3a**, where these bond angles are 83.94(7)° and 82.01(9)°, respectively. This is probably caused by the two relatively bulky groups, *i.e.*, dmso or PPh_3, and the isopropyl phenyl groups, being *cis* to each other, forming an angle N(1)–Pt(1)–S(1) of 97.35(7)° in **1a**, and angle N(11)–Pt(2)–P(24) of 103.50(9) in **3a**, and consequently resulting in a reduced angle O–Pt–Cl.

The steric effect of the ligand on the molecular structure is significant. In the case of ligand $\mathbf{L_A}$, the atoms of the metal-containing ring adopt a practically planar arrangement, as shown by the sum of their internal bond angles of *ca.* 720°.[20] With reduction of the steric bulk in **2**, a certain degree of strain of the metal-containing ring is observed with a sum of internal angles of 702.5°. In addition, a nearly facial (perpendicular) orientation[21] of the 2,6-diisopropyl phenyl ring to the metal-containing ring is observed in the complexes with the bulky ligand $\mathbf{L_A}$, as indicated by the torsion angle between the two planes around 90°, while, this angle is observed to decrease to 46.9(3)° in **2**, *i.e.*, the alternative edge (parallel) and facial arrangement does not exist in this case.

The *trans* influence of different ligands around the platinum centre can be compared by analysing the selected bond lengths for the *cis*/*trans* isomers, **1a**/**1b** and **3a**/**3b**. For dmso-ligated complexes, the Pt–$O(1)_{trans\text{-}S}$ bond length in *cis* **1a** [2.015(2) Å] is slightly longer than that *trans* to a chloride ligand, *i.e.*, Pt–$O(1)_{trans\text{-}Cl}$ in *trans* **1b** [1.991(2) Å], indicating the higher *trans* influence of dmso compared to that of Cl.[22] The longer Pt–$S(1)_{trans\text{-}N}$ [2.2304(8) Å] in *trans* **1b** than the Pt–$S(1)_{trans\text{-}O}$ in *cis* analogues **1a** [2.2181(8) Å] reveals the higher

Table 2 Crystal data and structure refinement for (salicylaldiminato)platinum(II) complexes **1–3**

	1a	**1b**	**2**	**3a**	**3b**
Empirical formula	$C_{21}H_{28}ClNO_2PtS + CH_2Cl_2$	$C_{21}H_{28}ClNO_2PtS$	$C_{15}H_{16}ClNO_2PtS$	$C_{37}H_{37}ClNOPPt + 2(CH_2Cl_2)$	$C_{37}H_{37}ClNOPPt$
M_r (g mol^{-1})	673.97	589.04	504.89	943.04	773.19
Crystal system	Triclinic	Monoclinic	Triclinic	Monoclinic	Monoclinic
Space group	$P\bar{1}$	$P2_1/c$	$P\bar{1}$	$P2_1/c$	$C2/c$
a (Å)	9.1719(3)	16.4013(18)	8.8183(2)	10.3272(9)	35.498(4)
b (Å)	11.1215(2)	19.269(2)	10.1831(2)	18.7983(17)	10.2831(11)
c (Å)	14.2096(4)	14.4597(16)	10.4630(2)	20.8684(18)	23.873(3)
α (°)	110.883(2)	90	111.9260(10)	90	90
β (°)	108.6750(10)	91.062(2)	93.0980(10)	100.185(2)	130.634(2)
γ (°)	91.334(2)	90	111.1600(10)	90	90
V (Å^3)	1267.38(6)	4569.0(9)	793.23(3)	3987.4(6)	6613.2(13)
Z	2	8	2	4	8
Reflections collected/unique	10 198/5197	10 6417/11 388	6569/3359	63 670/7573	61 047/9659
R (int)	0.0251	0.0618	0.0095	0.024	0.032
Data/restraints/parameters	5197/0/272	11 388/0/487	3359/0/191	7573/0/431	9659/0/383
Final R indices [$I > 2\sigma(I)$]	0.0239, 0.0411	0.0247, 0.0460	0.0144, 0.0325	0.0264, 0.0681	0.0191, 0.0444
Largest diff. peak and hole (e Å^{-3})	2.272, −0.903	0.888, −1.057	1.292, −0.764	1.60, −1.56	−0.52, 1.26
CCDC number	931185	931186	931187	931188	931189

Table 3 Selected bond lengths (Å), bond angles (°) and torsion angles (°) for (salicylaldiminato)platinum(II) complexes **1–3**

1a[a]		**1b**		**2**[a]		**3a**[a]		**3b**	
			(B)[b]						
Pt(1)–O(1)	2.015(2)	Pt(1)–O(1)	1.992(2)	Pt(1)–O(1)	2.019(18)	Pt(2)–O(3)	2.042(3)	Pt(1)–O(3)	2.001(2)
Pt(1)–N(1)	2.040(3)	Pt(1)–N(1)	2.029(3)	Pt(1)–N(1)	2.029(2)	Pt(2)–N(11)	2.021(3)	Pt(1)–N(11)	2.0707(2)
Pt(1)–S(1)	2.2181(8)	Pt(1)–S(1)	2.2304(8)	Pt(1)–S(1)	2.2062(6)	Pt(2)–P(24)	2.2586(9)	Pt(1)–P(24)	2.2566(7)
Pt(1)–Cl(1)	2.3118(8)	Pt(1)–Cl(1)	2.2961(9)	Pt(1)–Cl(1)	2.2981(16)	Pt(2)–Cl(1)	2.3174(9)	Pt(1)–Cl(2)	2.2993(8)
N(1)–C(7)	1.300(4)	N(1)–C(7)	1.292(4)	N(1)–C(1)	1.297(3)	N(11)–C(10)	1.301(5)	N(11)–C(10)	1.297(3)
		O(2)···H(2)[c]	2.22(4)						
O(1)–Pt(1)–N(1)	90.26(10)	O(1)–Pt(1)–N(1)	92.17(9)	O(1)–Pt(1)–N(1)	89.01(8)	O(3)–Pt(2)–N(11)	90.57(12)	O(3)–Pt(1)–N(11)	91.75(8)
O(1)–Pt(1)–S(1)	172.36(7)	O(1)–Pt(1)–S(1)	87.52(7)	O(1)–Pt(1)–S(1)	172.56(6)	O(3)–Pt(2)–P(24)	165.90(9)	O(3)–Pt(1)–P(24)	87.73(6)
N(1)–Pt(1)–Cl(1)	174.13(8)	N(1)–Pt(1)–Cl(1)	92.98(7)	N(1)–Pt(1)–Cl(1)	173.87(6)	N(11)–Pt(2)–Cl(1)	172.38(9)	N(11)–Pt(1)–Cl(2)	91.10(7)
S(1)–Pt(1)–Cl(1)	88.46(3)	S(1)–Pt(1)–Cl(1)	87.85(3)	S(1)–Pt(1)–Cl(1)	89.39(2)	P(24)–Pt(2)–Cl(1)	85.95(3)	P(24)–Pt(1)–Cl(2)	89.45(2)
N(1)–Pt(1)–S(1)	97.35(7)	N(1)–Pt(1)–S(1)	174.58(7)	N(1)–Pt(1)–S(1)	95.19(6)	N(11)–Pt(2)–P(24)	103.50(9)	N(11)–Pt(1)–P(24)	178.90(5)
O(1)–Pt(1)–Cl(1)	83.94(7)	O(1)–Pt(1)–Cl(1)	172.70(7)	C(1)–Pt(1)–Cl(1)	86.87(6)	O(3)–Pt(2)–Cl(1)	82.01(9)	O(3)–Pt(1)–Cl(2)	176.92(6)
C(7)–N(1)–Pt(1)	121.8(3)	C(7)–N(1)–Pt(1)	123.3(2)	C(11)–N(1)–Pt(1)	121.41(18)	C(10)–N(11)–Pt(2)	122.5(3)	C(10)–N(11)–Pt(1)	122.5(2)
C(1)–O(1)–Pt(1)	126.1(2)	C(1)–O(1)–Pt(1)	126.8(2)	C(7)–O(1)–Pt(1)	119.21(16)	C(4)–O(3)–Pt(2)	127.3(3)	C(4)–O(3)–Pt(1)	127.2(2)
O(1)–C(1)–C(6)	124.1(3)	O(1)–C(1)–C(6)	124.6(3)	O(1)–C(7)–C(2)	124.2(2)	O(3)–C(4)–C(9)	123.6(4)	O(3)–C(4)–C(9)	125.2(3)
C(1)–C(6)–C(7)	122.5(3)	C(1)–C(6)–C(7)	124.2(3)	C(7)–C(2)–C(1)	122.2(2)	C(4)–C(9)–C(10)	123.0(3)	C(4)–C(9)–C(10)	124.5(2)
N(1)–C(7)–C(6)	129.8(3)	N(1)–C(7)–C(6)	128.0(3)	N(1)–C(1)–C(2)	126.4(2)	N(11)–C(10)–C(9)	130.4(4)	N(11)–C(10)–C(9)	128.7(2)
Total 1[d]	360.0	Total 1[d]	360.5	Total 1[d]	360.5	Total 1[d]	360.0	Total 1[d]	360.0
Total 2[e]	714.6	Total 2[e]	719.1	Total 2[e]	702.5	Total 2[e]	717.5	Total 2[e]	720.0
Pt(1)–N(1)–C(8)–C(13)	−104.7(3)	Pt(1)–N(1)–C(8)–C(13)	−82.8(3)	Pt(1)–N(1)–C(8)–C(13)	46.9(3)	Pt(2)–N(11)–C(12)–C(13)	108.0(3)	Pt(1)–N(11)–C(12)–C(13)	−94.70(2)

[a] L is *cis* to N atom (L = dmso). [b] Molecule B. [c] Intermolecular interactions. [d] Sum of angles in the coordination environment of the platinum atom. [e] Sum of internal angles of the metal-containing ring.

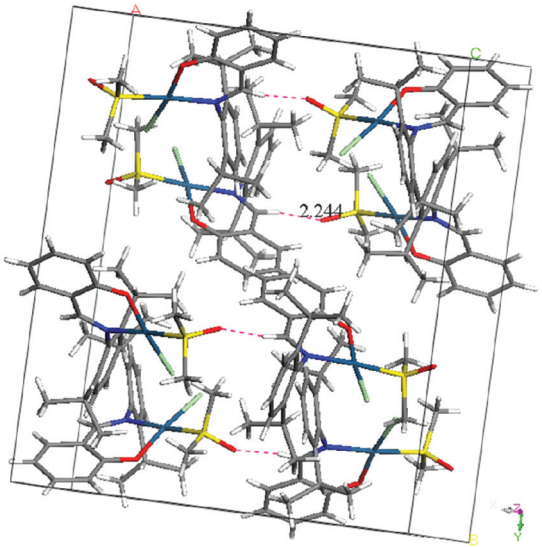

Fig. 9 Projection viewed along [010] for **1b**.

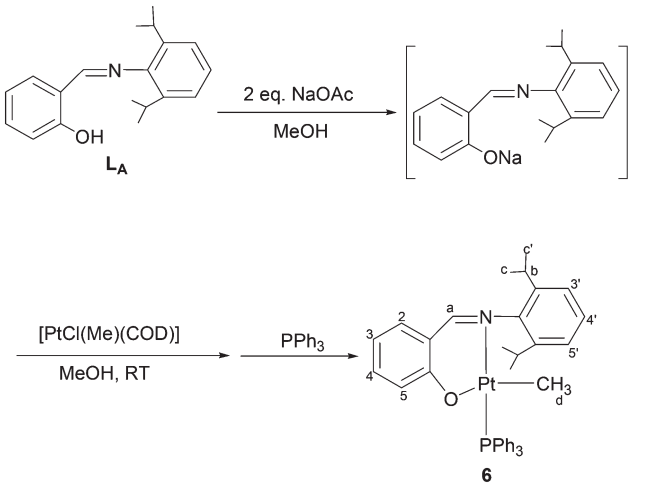

Scheme 3 Preparation of salicylaldiminato methylplatinum(II) complex **6**.

trans influence of the imine nitrogen as compared to the phenoxy oxygen atom of the N^O ligands.[23] This is also confirmed by the Pt–Cl bond lengths for the *cis*/*trans* complexes with either dmso or PPh_3 ligands, *i.e.*, Pt–Cl(1)$_{trans\text{-}N}$ in *cis* **1a**/**3a** > Pt–Cl(1)$_{trans\text{-}O}$ in *trans* **1b**/**3b**. Furthermore, there is slight lengthening of the Pt–N bond by 0.042 Å for the *trans* compound **3b** as compared to its dmso precursor **1b**, due to the higher *trans* effect of the P-donor ligand compared to that of the S-donor ligand.[24] The lengthening of the Pt–N distance agrees with the down-field shift of the imine proton in the ^{1}H NMR spectra for these complexes.

Intermolecular interaction is found in the *trans* complex **1b**. As shown in Fig. 9, the imino hydrogen in **1b** is involved in an interaction with the oxygen atom in the dmso ligand, N═CH···O (d(H(7A)···O(1B)) = 2.24(4) Å), increasing the stability of **1b** as previously suggested for analogous compounds.[25] No intermolecular interactions are found for the *cis* complexes or the PPh_3 derivatives.

Methylplatinum(II) salicylaldiminato complex

It has been mentioned above, that the "initiator complexes" involved in the reaction mechanisms for the chain propagation step in olefin oligomerization/polymerization using salicylaldiminato catalysts can have *cis* or *trans* configurations, in which the *cis* isomers (with the alkyl group *cis* to nitrogen) are more stable.[8,9] Herein, we report the synthesis of a model platinum "initiator complex", where R is a methyl group, to evaluate the stability of the *cis* isomer. The reaction of ligand $\mathbf{L_A}$ with [PtCl(cod)Me] was studied and the resulting compound, the salicylaldiminato methylplatinum(II) complex **6** is depicted in Scheme 3. The first step involves the reaction of the ligand precursor with 2 equivalents of sodium acetate, leading to deprotonation of the hydroxyl group to afford the sodium salt of the ligand *in situ*. Addition of equimolar amounts of [PtCl(cod)Me] and PPh_3 to the reaction mixture gave a yellow precipitate, consisting of a mixture of **6** and a small amount of the by-product *trans*-[PtCl(Me)$(PPh_3)_2$]. Column chromatography on SiO_2 yielded the pure target complex, **6**.

For the methylplatinum(II) complex **6**, the *cis* arrangement of the methyl group and the imine is expected, and this is confirmed by the experimental evidence, where coupling of both the imine proton to the phosphorus ($^4J_{P-H}$ = 12.2 Hz, Table 1), and the coupling of the imine proton to platinum ($^3J_{Pt-H}$ = 70.9 Hz) in a *trans* position is observed in the ^{1}H NMR spectrum. As shown in Fig. 3, the ^{1}H NMR spectra of **6** is almost identical to that of **3b** which has the imine nitrogen *trans* to PPh_3. In the case of complex **6**, however, an additional resonance for the methyl group on platinum appears as a doublet of doublets at −0.29 ppm. In fact, all previously reported salicylaldiminato methylpalladium complexes have a *cis* geometry in which the methyl group is *cis* to the N atom.[18,26]

cis–*trans* Isomerization of 3a

We have noticed when triphenylphosphine is added to a solution of **1a** or **1b**, the kinetically controlled product **3a** with phosphorus coordinating *cis* to the imine group is obtained. On heating, the kinetic product **3a** undergoes a slow conversion to the thermodynamically more stable *trans* complex **3b**, resulting in an up-field resonance at 6.31 ppm ascribed to the H^5 proton, as well as a change in both the Pt–P and Pt–H coupling constants. In particular, the Pt–P coupling constant changes from 4063 to 3818 as a result of the isomerization of the PPh_3 from the *cis* to the *trans* position.

According to DFT calculations on salicylaldiminato Ni/Pd catalyzed olefin polymerization, tetrahedral transition states have been found for *cis*–*trans* isomerization of four-coordinated complexes. The (salicylaldiminato)platinum(II) systems under investigation here allow us to determine kinetic and computational data for the *cis*–*trans* isomerization **3a** → **3b** (eqn (1)), and to evaluate the possible mechanism for the isomerization process.

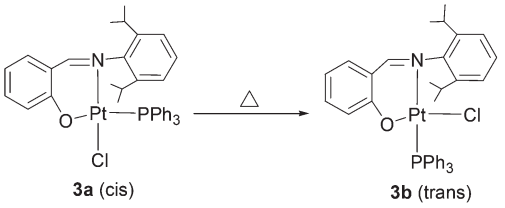

(1)

Kinetics of the *cis–trans* isomerisation

The *cis–trans* geometrical conversion **3a** → **3b** in $CDCl_3$ was investigated quite easily in the temperature range 313–336 K using ^{31}P NMR spectroscopy. In this temperature range, the conversion is *ca.* 95%, yielding the stable *trans* isomer and a small amount of the starting *cis* isomer at the end of the reaction. The reaction rate was determined from the NMR data and found to be pseudo-first-order. The rate constants at different temperatures are given in Table 4.

The progress of each reaction was monitored by following the decrease of the ^{31}P resonance at −2.14 ppm associated with **3a**. Fig. 10 shows the spectral changes during the transformation **3a** → **3b** at 338 K. The two clearly defined resonances at 8.67 and −2.37 ppm are an indication that the isomerization is well-behaved and is free of kinetic complications. The pseudo-first-order plots for the transformation of **3a** to **3b** at different temperatures are depicted in Fig. 11(A).

Table 4 Experimental pseudo-first-order rate constants for the isomerization of **3a** to **3b**

Entry	*T*/K	$k_{obs}/10^{-5}$ s^{-1}
1	313	0.19 ± 0.01
2	320	0.43 ± 0.02
3	328	1.39 ± 0.06
4	336	3.85 ± 0.12

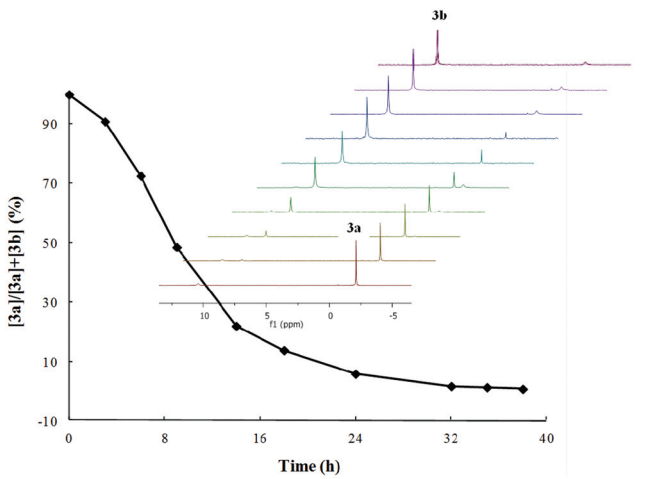

Fig. 10 The relative intensity of the **3b** resonance *versus* time plot for the experimental data at 338 K (solid black line). Inside: ^{31}P NMR spectral changes associated with the geometrical isomerization of **3a** to **3b** in $CDCl_3$ at 338 K.

The variable-temperature rate constants for the isomerization reaction listed in Table 4 were fitted to the Eyring equation (see eqn (2) in Experimental section) and yielded $\Delta H^{\ddagger}$ = 26.9 ± 1.1 kcal mol^{-1}, $\Delta S^{\ddagger}$ = 1.2 ± 3.3 eu and $\Delta G^{\ddagger}_{298.15}$ = 26.6 ± 0.1 kcal mol^{-1} [Fig. 11(B)]. The value of $\Delta H^{\ddagger}$ obtained is comparable with that of similar systems,[27] while the value of $\Delta S^{\ddagger}$ is known to vary with different isomerization mechanisms.[28]

Theoretical calculations

The possible mechanisms for *cis–trans* isomerization depend on the nature of the solvent, the electronic nature of the ligands and the temperature.[29] Different mechanisms usually considered for *cis–trans* isomerization in square-planar complexes include the associative pathway,[30] the Berry pseudo-rotation mechanism,[31] the dissociative pathway,[32] and direct geometry change *via* a tetrahedral four-coordinate transition state.[33]

Both the associative and Berry pseudo-rotation mechanisms need the coordination of a fifth ligand such as an extra PR_3 ligand, an ethylene or a solvent molecule.[31a,34] In our system, solvent is the only possible source of the fifth ligand. Since $CDCl_3$ is a non-coordinating solvent, we can rule out these two pathways involving five-coordinate intermediates. Therefore, both the dissociative and the direct geometry change pathways could be possible mechanisms for the isomerization process of **3a** to **3b**. In addition, both the dissociation of PPh_3 and the dissociation of the N-atom of the hemilabile imine ligand could be possible for the dissociative pathway. Three isomerization routes were therefore investigated. The energy profiles are shown in Fig. 12 and the calculated activation parameters as well as the experimental values are given in Table 5. Fig. 13 shows the optimized structures of the stationary points of Fig. 12.

Our computational studies were carried out by performing DFT calculations on the isomerization of **3a** through the dissociative pathway, involving the dissociation of the PPh_3 ligand, as well as the direct geometry change *via* a tetrahedral four-coordinate transition state. It is worth noting that both the "Y-shaped" three-coordinate transition state (TS-P) and the tetrahedral four-coordinate transition state (TS) were determined to be extremely close in activation energy ($\Delta G^{\ddagger}_{298.15}$), in which TS-P is about 2 kcal mol^{-1} more stable than TS (see Table 5). On the other hand, TS-P is 10.6 kcal mol^{-1} higher in enthalpy ($\Delta H^{\ddagger}_{298.15}$) than TS, due to the very positive value of $\Delta S^{\ddagger}$ for TS-P (45.3 eu), which is expected for the dissociative mechanism.[27a,28b] Thus, the small experimental value of $\Delta S^{\ddagger}$ obtained (1.2 ± 3.3 eu) does not correspond to the calculated $\Delta S^{\ddagger}$ for the dissociation of PPh_3 (45.3 eu), and thus we can rule out this mechanism.

The third route proposed for isomerization of **3a** is the dissociative pathway involving the dissociation of the imine N. The dissociation of the labile imine N from **3a** affords a *cis*-like three-coordinate intermediate, **3a-N**, with an agostic interaction between the Pt centre and the imine hydrogen (Pt···H distance is 2.467 Å). As shown in Fig. 12, conversion of an agostic "*cis*-like" three-coordinate form to its *trans* form **3b-N**

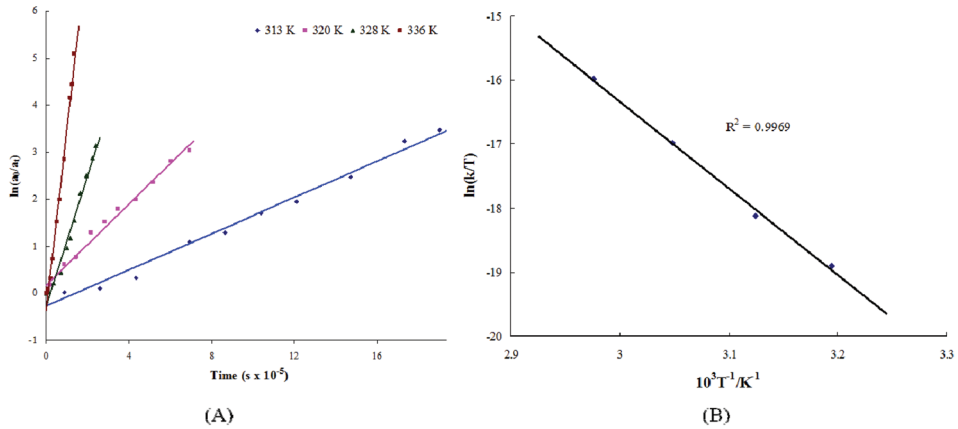

Fig. 11 (A) The pseudo-first-order plots for *cis–trans* isomerization of **3a** at variable-temperature. (B) Eyring plot for the isomerization reaction of **3a** constructed by the use of rate data obtained from ^{31}P NMR experiments.

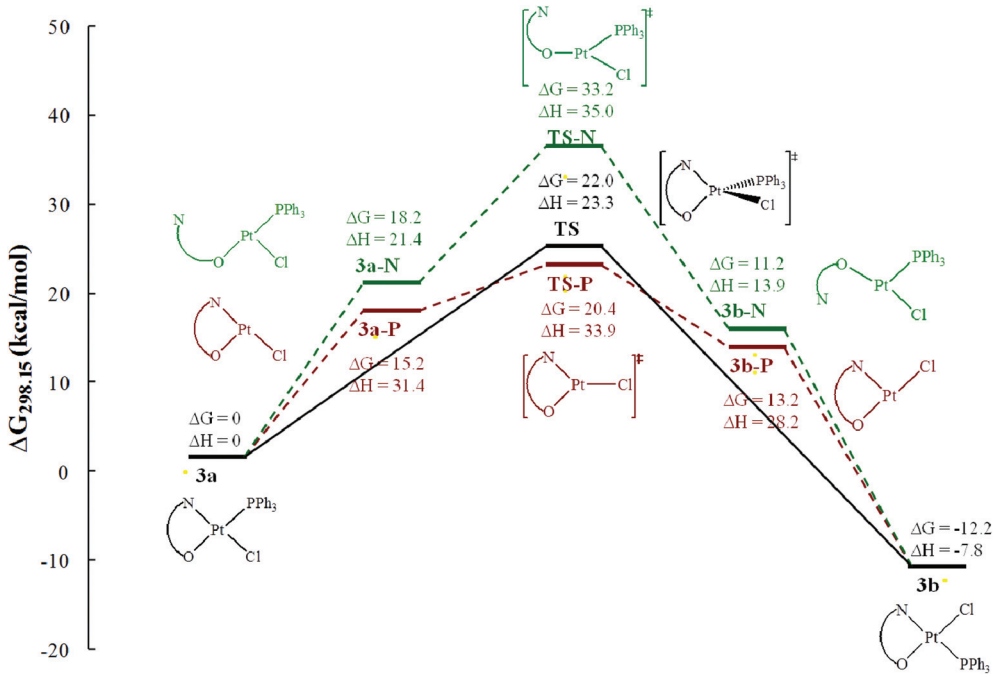

Fig. 12 Isomerization routes: simple rotation *via* tetrahedral TS (black), dissociative route *via* the dissociation of PPh_3 (red) and dissociative route *via* the dissociation of N atom (green). ($\Delta G_{298.15}/\Delta H_{298.15}$, kcal mol^{-1} at 1 atm relative to **3a**).

Table 5 Summary of theoretical and kinetic data for the *cis–trans* isomerization of **3a**

Entry	$\Delta H^{\ddagger}_{298.15}$ (kcal mol^{-1})	$\Delta S^{\ddagger}_{298.15}$ (eu)	$\Delta G^{\ddagger}_{298.15}$ (kcal mol^{-1})
1[a]	33.9	45.3	20.4
2[b]	35.0	−6.1	33.2
3[c]	23.3	4.1	22.0
4[d]	26.9 ± 1.1	1.2 ± 3.3	26.6 ± 0.1

[a] Dissociative mechanism via the dissociation of the PPh_3 ligand. [b] Dissociative mechanism via the dissociation of the N-atom. [c] One-step, direct geometry change mechanism. [d] Experimental values.

requires additional consumption of energy. Our calculations find that TS-N is the highest energy transition structure of the three isomerization routes, and is higher in both enthalpy and activation energy (*ca.* 11 kcal mol^{-1}) thus making the imine dissociation a less likely pathway compared to the one involving the tetrahedral transition state, TS.

Therefore, the calculated activation parameters of $\Delta H^{\ddagger}$ = 23.3 kcal mol^{-1}, $\Delta S^{\ddagger}$ = 4.1 eu for the isomerization of **3a** to **3b** *via* the tetrahedral four-coordinate transition state (TS) are in good agreement with the experimental values of $\Delta H^{\ddagger}$ = 26.9 ± 1.1 kcal mol^{-1}, $\Delta S^{\ddagger}$ = 1.2 ± 3.3 eu (see Table 5). This

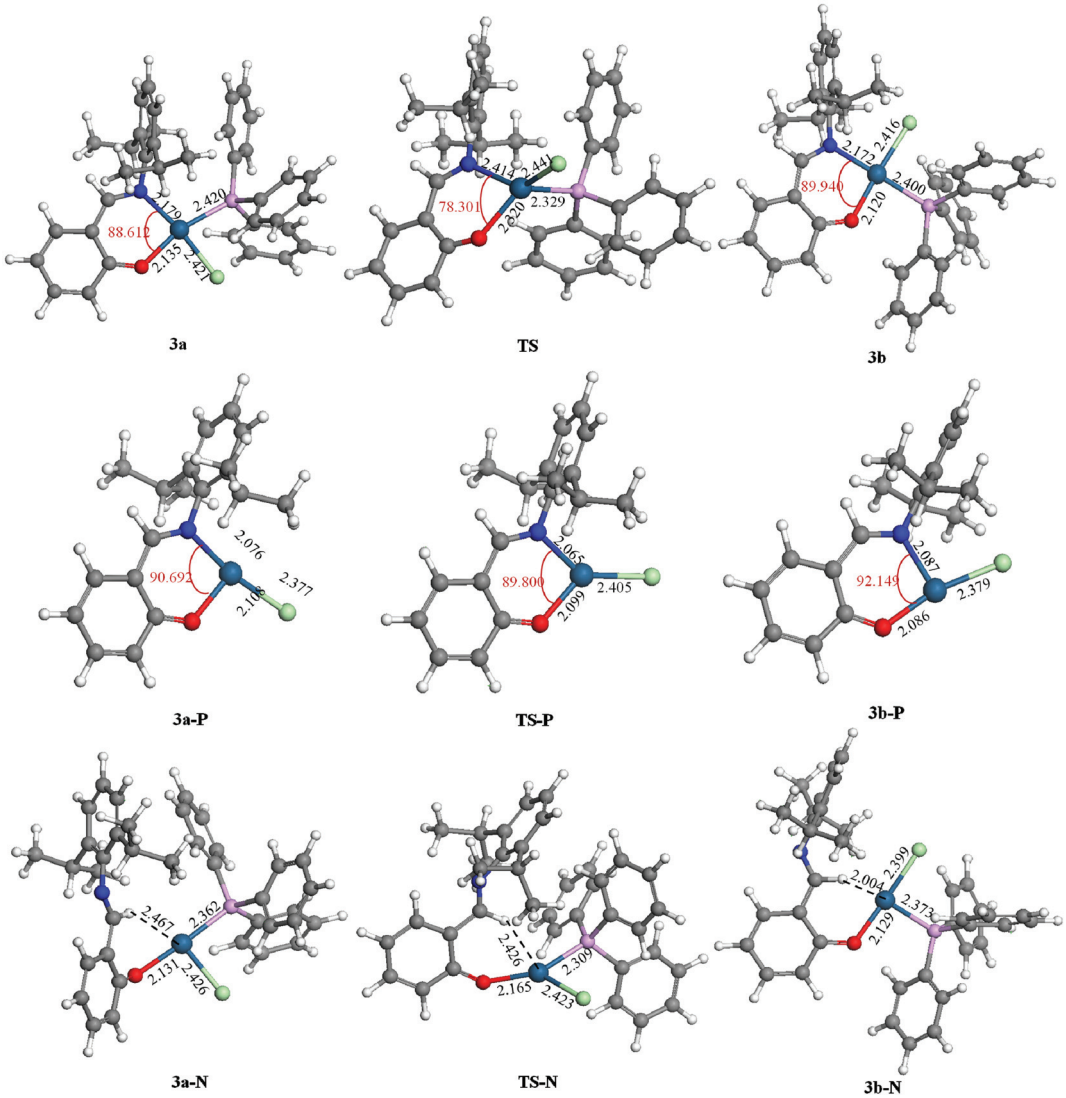

Fig. 13 Fully optimized geometrical structures of stationary points intercepted along the energy profile for isomerization of complex **3a**. Bond lengths are in angstroms and angles in degrees.

agreement provides support for the computational finding that the one-step, direct geometry change mechanism is really preferred to the three-step dissociative mechanism, and agrees with the DFT findings on *cis–trans* isomerization of related salicylaldiminato complexes *via* tetrahedral transition states.[9]

Conclusions

The preparation of novel (salicylaldiminato)platinum(II) complexes has been achieved by reacting *cis*-[$PtCl_2(dmso)_2$] with two salicylaldimine ligands of different steric bulk. This allowed for a comparative study of their structures and reactivity. The steric effect of the salicylaldiminato ligands seems to play an important role in their coordination behaviour leading to the specific molecular structures obtained for the complexes.

In the case of the dmso complexes, reaction with PPh_3 occurs readily to bring about the displacement of the dmso ligand. However, in the case of reactions with the diphosphines (dppf and dppe) the success of the reaction is dependent on the backbone of diphosphines and the configuration of the dmso-ligated precursors.

cis-Methylplatinum(II) complex **6** was obtained as a single isomeric product from an alternative route using [PtCl(Me)(cod)] as starting material, indicating that the (salicylaldiminato)platinum(II) complex with R group (R = Me) *cis* to the imine nitrogen is more stable.

The *cis–trans* isomerization of the N^O complex **3a** was studied both experimentally and theoretically. The results of DFT calculations suggest that a direct geometry change mechanism *via* a tetrahedral transition state would be the most likely *cis–trans* isomerization pathway amongst the studied mechanisms. The computed activation parameters are in very

good agreement with the experimental activation parameters obtained from kinetic studies.

Experimental section

General

The solvents were purified and distilled using standard methods. Anhydrous HPLC grade methanol (dry, max. 0.005% H_2O) was purchased from Aldrich.

NMR spectra were recorded on a Varian Mercury-300 MHz or Varian Unity-400 MHz spectrometer. Residual solvent signals were used as reference for ^1H and ^{13}C NMR. H_3PO_4 (85% in D_2O) were used as reference for ^{31}P NMR. Abbreviations used: s = singlet, d = doublet, t = triplet, m = multiplet, b = broad, NMR labelling is as shown in Schemes 1–3. Infrared spectra were recorded as KBr pellets and measured on a Perkin Elmer Spectrum One FT-IR spectrophotometer. Mass spectral analyses were carried out at Stellenbosch University on a Waters Q-TOF Ultima API or Waters Quattro Micro API mass spectrometer and using the electrospray ionization technique. Elemental analyses were carried out on a Fisons EA 1108 CHNS Elemental Analyzer at the microanalytical laboratory of the University of Cape Town. Melting points were recorded on a Kofler hotstage microscope (Reichert Thermovar).

X-ray single crystal intensity data for structures were collected on Nonius Kappa-CCD (**1a**, **1b** and **2**) or Bruker KAPPA APEX II DUO (**3a** and **3b**) diffractometers using graphite monochromated MoKα radiation (λ = 0.71073 Å). The temperature was controlled by an Oxford Cryostream cooling system (Oxford Cryostat). The strategy for the data collections was evaluated using the Bruker Nonius "Collect" program. Data were scaled and reduced using DENZO-SMN software.[35] An empirical absorption correction using the program SADABS[36] was applied. The structure was solved by direct methods and refined employing full-matrix least-squares with the program SHELXL-97,[37] refining on F^2. Packing diagrams were produced using the program PovRay and the graphic interface X-Seed.[38] All the non-hydrogen atoms were refined anisotropically. The hydrogen atoms were placed in idealised positions in a riding model with U_{iso} set at 1.2 or 1.5 times those of their parent atoms and fixed C–H bond lengths.

Preparation of the compounds

The starting material *cis*-$[PtCl_2(SOMe_2)_2]$[39] and salicylaldiminato ligands $\mathbf{L_A}$–$\mathbf{L_B}$[2a] were prepared as reported elsewhere.

[PtCl{(OC$_6$H$_4$)CH=N{2,6-(Me$_2$CH)$_2$(C$_6$H$_3$)}}(SOMe$_2$)] (1). *cis*-$[PtCl_2(SOMe_2)_2]$ (0.522 g, 1.24 mmol) and the imine $\mathbf{L_A}$ (0.348 g, 1.24 mmol) in the presence of sodium acetate (0.101 g, 1.24 mmol) were allowed to react in dry methanol (20 ml) under reflux for 2 h. The solvent was removed on a rotary evaporator, and the residue obtained was dissolved in a minimum amount of CH_2Cl_2 and then passed through a SiO_2 column. Two isomeric forms of this product (**1a** and **1b**) were isolated. *n*-Hexane–ethyl acetate (95 : 5) was used to elute the unreacted ligand (first band) while the second band was eluted using *n*-hexane–ethyl acetate (70 : 30), to isolate complex **1a**. The third band was eluted by *n*-hexane–ethyl acetate (50 : 50) solution to give isomer **1b**. These isomers differ in the position of the Cl^- ligand [*trans* to N atom (**1a**) or O atom (**1b**)].

1a, yield 0.550 g, 75%. M.p.: 165–167 °C. IR (KBr): ν(CH=N) 1606 cm^{-1}, (S=O) 1154 cm^{-1}. ^1H NMR (300 MHz, $CDCl_3$): δ = 7.73 [s, $^3J_{Pt-H}$ = 93.27 Hz, 1H, H^a], 7.43 [dd, $^3J_{H-H}$ = 8.53 Hz, $^4J_{H-H}$ = 1.60 Hz, 1H, H^2], 7.24 [t, $^3J_{H-H}$ = 7.74 Hz, 1H, H4′], 7.13 [d, $^3J_{H-H}$ = 8.34 Hz, 2H, H^{3,4}], 7.07 [d, $^3J_{H-H}$ = 7.74 Hz, 2H, H$^{3',5'}$], 6.63 [dd, $^3J_{H-H}$ = 7.33 Hz, $^4J_{H-H}$ = 1.86 Hz, 1H, H^5], 3.32 [s, 6H, H^d], 3.51 [hept, 2H, H^b], 1.28 [d, $^3J_{H-H}$ = 6.88 Hz, 6H, H^c], 1.03 [d, $^3J_{H-H}$ = 6.79 Hz, 6H, H$^{c'}$]. ^{13}C NMR ($CDCl_3$): δ = 163.05 [s, C^a], 162.47 [s, C$^{1'}$], 148.19 [s, C^6], 141.78 [s, C$^{2',6'}$], 136.68 [s, C^2], 133.66 [s, C^3], 128.00 [s, C$^{4'}$], 123.37 [s, C$^{3',5'}$], 123.06 [s, C^6], 120.79 [s, C^4], 117.25 [s, C^5], 47.37 [s, C^d], 27.93 [s, C^b], 24.71 [s, C$^{c'}$], 22.54 [s, C^c]. EI-MS: *m*/*z* 590.12 [M]$^+$, 556.18 [M − OMe]$^+$, 553.15 [M − Cl]$^+$, 515.15 [M − ^{i}Pr − Me]$^+$, 474.12 [M − Cl − dmso]$^+$. Anal. found (calc. for $C_{21}H_{28}ClNO_2PtS$): C: 43.08 (42.82), H: 4.92 (4.79), N: 2.26 (2.59), S: 5.19 (5.43).

1b, yield 0.164 g, 23%. M.p.: 193–195 °C. IR: ν (CH=N) 1606 cm^{-1}, (S=O) 1140 cm^{-1}. ^1H NMR (300 MHz, $CDCl_3$): δ = 7.73 (s, $^3J_{Pt-H}$ = 59.47 Hz), 7.73 [s, $^3J_{Pt-H}$ = 93.27 Hz, 1H, H^a], 7.41 [dd, $^3J_{H-H}$ = 8.68 Hz, $^4J_{H-H}$ = 1.81 Hz, 1H, H^2], 7.20 [t, $^3J_{H-H}$ = 7.74 Hz, 1H, H$^{4'}$], 7.15–7.09 [m, 2H, H^{3,4}], 7.04 [dd, $^3J_{H-H}$ = 8.67 Hz, $^4J_{H-H}$ = 0.54 Hz, 2H, H$^{3',5'}$], 6.65 [dd, $^3J_{H-H}$ = 7.96 Hz, $^4J_{H-H}$ = 1.08 Hz, 1H, H^5], 3.32 [s, 6H, H^d], 3.26 [hept, 2H, H^b], 1.27 [d, $^3J_{H-H}$ = 6.80 Hz, 6H, H^c], 1.03 [d, $^3J_{H-H}$ = 6.88 Hz, 6H, H$^{c'}$]. ^{13}C NMR ($CDCl_3$): δ = 162.83 [s, C$^{1'}$], 161.45 [s, C^a], 146.36 [s, C^6], 141.78 [s, C$^{2',6'}$], 136.09 [s, C^2], 134.38 [C^3], 127.66 [C$^{4'}$], 123.38 [s, C^1], 123.07 [C$^{3',5'}$], 120.62 [s, C^4], 117.11 [s, C^5], 42.31 [s, C^d], 28.09 [s, C^b], 24.40 [s, C$^{c'}$], 22.79 [s, C^c]. EI-MS: *m*/*z* 590.12 [M]$^+$, 556.18 [M − OMe]$^+$, 553.15 [M − Cl]$^+$, 515.15 [M − ^{i}Pr − Me]$^+$, 474.12 [M − Cl − dmso]$^+$. Anal. found (calc. for $C_{21}H_{28}ClNO_2PtS$): C: 43.07 (42.82), H: 4.86 (4.79), N: 2.38 (2.59), S: 5.45 (5.43).

[PtCl{(OC$_6$H$_4$)CH=N(C$_6$H$_5$)}(SOMe$_2$)] (2). *cis*-$[PtCl_2(SOMe_2)_2]$ (0.540 g, 1.28 mmol) and the imine $\mathbf{L_B}$ (0.252 g, 1.28 mmol) in the presence of sodium acetate (0.105 mg, 1.28 mmol) were allowed to react in dry methanol (20 ml) for 16 h at room temperature. A yellow precipitate of complex **2** formed. The product was collected by filtration *in vacuo*. Yield: 0.435 g, 67%. M.p.: 170–172 °C. IR (KBr): ν (CH=N) 1607 cm^{-1}, (S=O) 1155 cm^{-1}. ^1H NMR (300 MHz, $CDCl_3$): δ = 7.83 [s, $^3J_{Pt-H}$ = 86.34 Hz, 1H, H^a], 7.47 [d, $^3J_{H-H}$ = 7.19 Hz, 2H, H$^{2',6'}$], 7.36 [m, 3H, H$^{3',4',5'}$], 7.27 [d, $^3J_{H-H}$ = 7.26 Hz, 1H, H^2], 7.21 [dt, $^3J_{H-H}$ = 8.08 Hz, $^4J_{H-H}$ = 1.30 Hz, 1H, H^4], 7.11 [t, $^3J_{H-H}$ = 8.60 Hz, 1H, H^3], 6.64 [d, $^3J_{H-H}$ = 7.42 Hz, 1H, H^5], 3.24 [s, 6H, H^d]. ^{13}C NMR (101 MHz, $CDCl_3$): δ = 163.47 [s, C$^{1'}$], 162.69 [s, C^a], 153.52 [s, C^6], 136.79 [s, C^2], 133.66 [s, C^4], 128.82 [s, C$^{2',6'}$], 128.00 [s, C$^{4'}$], 124.18 [s, C$^{3',5'}$], 121.06 [s, C^3], 120.08 [s, C^1], 117.58 [s, C^5], 46.36 [s, C^d]. EI-MS: *m*/*z* 506.03 [M]$^+$, 469.05 [M − Cl]$^+$, 391.04 [M − Cl − Ph]$^+$, 390.04 [M − Cl − dmso]$^+$. Anal. found (calc. for $C_{15}H_{16}ClNO_2PtS$): C, 35.90 (35.68); H, 3.02 (3.19); N, 2.38 (2.77), S 5.98 (6.35).

[PtCl{(OC$_6$H$_4$)CH═N{2,6-(Me$_2$CH)$_2$(C$_6$H$_3$)}}(PPh$_3$)] (3). **1a** or **1b** or the mixture of **1a** and **1b** (0.566 g, 1.0 mmol) and triphenylphosphine (0.296 g, 1.0 mmol) were allowed to react in dichloromethane (20 ml) at room temperature for 2 h. The solvent was removed using a rotary evaporator, and the residue obtained was dissolved in a minimum amount of CH_2Cl_2 and then passed through a SiO_2 column. Two isomeric forms of this product (**3a** and **3b**) were isolated. Elution with *n*-hexane–ethyl acetate (98 : 2) solution produced a yellow band, which yielded **3b**; elution with *n*-hexane–ethyl acetate (80 : 20) solution yielded a second band that was collected and concentrated to give **3a**. These isomers differ in the coordination site of the PPh_3 ligand [*cis* to N atom (**3a**) or *trans* to N atom (**3b**)].

3a, yield 0.294 mg, 34%. M.p.: 212–214 °C. IR: ν (CH═N) 1606 cm^{-1}. ^{1}H NMR (300 MHz, $CDCl_3$): δ = 7.61 [s, 1H, H^a], 7.49 [d, $^3J_{H-H}$ = 8.32 Hz, 1H, H^2], 7.48–7.43 [m, 6H, Ph–H], 7.29–7.25 [m, 3H, Ph–H], 7.19 [d, $^3J_{H-H}$ = 8.76 Hz, 1H, H^5], 7.16–7.12 [m, 6H, Ph–H], 7.09 [dt, $^3J_{H-H}$ = 8.07 Hz, $^4J_{H-H}$ = 1.48 Hz, 1H, H^4], 6.83 [t, $^3J_{H-H}$ = 7.77 Hz, 1H, H$^{4'}$], 6.64 [d, $^3J_{H-H}$ = 7.75 Hz, 2H, H$^{3',5'}$], 6.59 [t, $^3J_{H-H}$ = 7.29 Hz, 1H, H^3], 3.66 [hept, 2H, H^b], 0.94–0.92 [m, 12H, H$^{c,c'}$]. ^{13}C NMR (101 MHz, $CDCl_3$): δ = 163.94 [s, C^a], 163.22 [s, C$^{1'}$], 151.50 [s, C^6], 140.99 [s, C$^{2',6'}$], 136.17 [s, C^2], 134.92 [d, J_{P-C} = 10.29, 6C, Ph–C], 133.48 [s, C^4], 129.83 [d, J_{P-C} = 2.33 Hz, 3C, Ph–C], 128.50 [s, C$^{4'}$], 127.81 [d, J_{P-C} = 11.05, 6C, Ph–C], 123.59 [s, C$^{3',5'}$], 122.05 [s, C^5], 118.85 [s, C^1], 116.25 [s, C^3], 27.78 [s, C^b], 25.48 [s, C$^{c'}$], 21.91 [s, C^c]. ^{31}P NMR (121 MHz, $CDCl_3$): δ = −2.14 [s, J_{P-Pt} = 4063.88]. EI-MS: *m*/*z* 774.2 [M]$^+$, 737.2 [M − Cl]$^+$. Anal. found (calc. for $C_{37}H_{37}ClNOPPt$): C, 57.70 (57.47); H, 5.02 (4.82); N, 1.73 (1.81).

3b, yield 0.423 g, 48%. M.p.: 236–238 °C. IR: ν (CH═N) 1609.8 cm^{-1}. ^{1}H NMR (300 MHz, $CDCl_3$): δ = 8.06 [d, $^4J_{P-H}$ = 13.92 Hz, 1H, H^a], 7.83–7.76 [m, 6H, Ph–H], 7.50 [d, $^3J_{H-H}$ = 13.92 Hz, 1H, H^2], 7.48–7.36 [m, 9H, Ph–H], 7.26 [t, $^3J_{H-H}$ = 1.82 Hz, 1H, H^4], 7.24 [t, $^3J_{H-H}$ = 1.80 Hz, 1H, H$^{4'}$], 7.20 [d, $^3J_{H-H}$ = 1.61 Hz, 2H, H$^{3',5'}$], 6.57 [dt, $^3J_{H-H}$ = 7.50 Hz, $^4J_{H-H}$ = 1.07 Hz, 1H, H^3], 6.31 [dd, $^3J_{H-H}$ = 8.57 Hz, $^4J_{H-H}$ = 0.49 Hz, 1H, H^5], 3.53 [hept, 2H, H^b], 1.41 [d, $^3J_{H-H}$ = 6.83 Hz, 6H, H^c], 1.14 [d, $^3J_{H-H}$ = 6.83 Hz, 6H, H$^{c'}$]. ^{13}C NMR (101 MHz, $CDCl_3$): δ = 163.46 [s, C$^{1'}$], 160.48 [s, C^a], 146.33 [s, C^6], 141.86 [s, C$^{2',6'}$], 135.13 [d, J_{P-C} = 10.52 Hz, 6C, Ph–C], 134.89 [s, C^2], 134.48 [s, C^4], 130.63 [d, J_{P-C} = 2.38 Hz, 3C, Ph–C], 128.71 [s, C^1], 127.85 [d, J_{P-C} = 11.11 Hz, 6C, Ph–C], 126.98 [s, C$^{4'}$], 122.84 [s, C$^{3',5'}$], 121.10 [s, C^5], 116.10 [s, C^3], 28.18 [s, C^b], 24.73 [s, C$^{c'}$], 22.86 [s, C^c]. ^{31}P NMR (121 MHz, $CDCl_3$): δ = 8.87 [s, J_{P-Pt} = 3818.82]. EI-MS: *m*/*z* 774.2 [M]$^+$, 737.2 [M − Cl]$^+$, Anal. found (calc. for $C_{37}H_{37}ClNOPPt$): C, 57.78 (57.47); H, 4.93 (4.82); N, 1.72 (1.81).

[PtCl{(OC$_6$H$_4$)CH═N(C$_6$H$_5$)}(PPh$_3$)] (4). Complex **4** was obtained from **2** (0.108 g, 0.21 mmol) and triphenylphosphine (56 mg, 0.21 mmol), which were allowed to react in dichloromethane (20 ml) at room temperature for 2 h. The solvent was removed on a rotary evaporator, and the residue obtained was dissolved in a minimum amount of CH_2Cl_2 and then passed through a SiO_2 column. Elution with an *n*-hexane–ethyl acetate (90 : 10) solution gave a yellow band. Yield 0.102 g (69.3%). M.p.: 210–212 °C. IR: ν (CH═N) 1608 cm^{-1}. ^{1}H NMR (300 MHz, $CDCl_3$): δ = 8.20 [d, $^4J_{P-H}$ = 13.39 Hz, 1H, H^a], 7.77 (m, 6H, Ph–H), 7.47 [d, $^3J_{H-H}$ = 6.84 Hz, 1H, H^2], 7.45–7.37 (m, 9H, Ph–H), 7.35 (m, 1H, H^4) 7.28 (d, $^3J_{H-H}$ = 7.48 Hz, 2H, H$^{2',6'}$), 7.22 (t, $^3J_{H-H}$ = 7.64 Hz, 2H, H$^{3',5'}$) 7.17 (t, $^3J_{H-H}$ = 8.60 Hz, 1H, H$^{4'}$), 6.55 (t, $^3J_{H-H}$ = 7.53 Hz, 1H, H^3), 6.16 (d, $^3J_{H-H}$ = 8.62 Hz, 1H, H^5). ^{13}C NMR (101 MHz, $CDCl_3$): δ = 163.01 [s, C$^{1'}$], 160.89 [s, C^a], 151.12 [s, C^6], 135.06 [d, J_{P-C} = 11.52 Hz, 6C, Ph–C], 134.96 [s, C$^{4'}$], 130. 67 [s, C$^{2,2',6'}$], 128.20 [d, J_{P-C} = 2.42 Hz, 3C, Ph–C], 127.96 [d, J_{P-C} = 10.32 Hz, 6C, Ph–C], 124.83 [s, C$^{3',5'}$], 121.86 [s, C^5], 119.64 [s, C^1], 116.52 [s, C^3]. ^{31}P NMR (121 MHz, $CDCl_3$): δ = 7.40 [s, J_{P-Pt} = 3869 Hz]. EI-MS: *m*/*z* 688.2 [M]$^+$, 653.8 [M − Cl]$^+$. Anal. found (calc. for $C_{31}H_{25}ClNOPPt$): C, 54.64 (54.04); H, 3.85 (3.66); N, 1.87 (2.03).

[{PtCl(OC$_6$H$_4$)CH═N{2,6-(Me$_2$CH)$_2$(C$_6$H$_3$)}}$_2$(μ-dppf)] (5). Complex **5** was obtained from compound **1b** (0.119 g, 0.202 mmol) and dppf (0.056 g, 0.1014 mmol) which were allowed to react in dichloromethane (20 ml) at room temperature for 16 h. The solvent was removed on a rotary evaporator, and the residue obtained was dissolved in a minimum amount of CH_2Cl_2 and then passed through a SiO_2 column. *n*-Hexane was used to elute the unreacted dppf, and the second band was removed by an *n*-hexane–ethyl acetate (95 : 5) mixture to produce complex **5**. Yield: 68 mg, (75%). M.p.: decompose without melting at 281–283 °C. IR (KBr): ν (CH═N) 1610 cm^{-1}. ^{1}H NMR (400 MHz, $CDCl_3$): δ = 8.03 [d, $^3J_{H-H}$ = 14.16 Hz, 2H, H^a], 7.67–7.58 [m, 8H, Ph–H], 7.41 [d, $^3J_{H-H}$ = 6.63 Hz, 2H, H^2], 7.39 [d, $^3J_{H-H}$ = 6.59 Hz, 4H, Ph–H], 7.35–7.25 [m, 8H, Ph–H], 7.22–7.20 [m, 2H, H^4], 7.18 [d, $^3J_{H-H}$ = 7.43 Hz, 4H, H$^{3',5'}$], 7.17–7.14 [m, 2H, H$^{4'}$], 6.53 [t, $^3J_{H-H}$ = 7.12 Hz, 2H, H^3], 6.14 [d, $^3J_{H-H}$ = 8.60 Hz, 2H, H^5], 4.74 [d, $^3J_{H-H}$ = 0.98 Hz, 4H, H^e], 4.63 [d, $^3J_{H-H}$ = 1.55 Hz, 4H, H^d], 3.67–3.33 [hept, 4H, H^b], 1.33 [d, $^3J_{H-H}$ = 6.81 Hz, 12H, H$^{c'}$], 1.08 [d, $^3J_{H-H}$ = 6.84 Hz, 1H, H^c]. ^{13}C NMR (101 MHz, $CDCl_3$): δ = 163.26 [s, C$^{1'}$], 160.68 [s, C^a], 146.39 [s, C^6], 141.98 [s, C$^{2',6'}$], 134.93 [s, C^2], 134.53 [s, C^6], 134.27 [d, J_{P-C} = 10.41 Hz, 8C, Ph–C], 130.33 [s, C$^{4'}$], 127.54 [d, J_{P-C} = 11.15 Hz, 12C, Ph–C], 127.01 [s, C^4], 122.85 [s, C$^{3',5'}$], 120.98 [s, C^5], 119.68 [s, C^1], 116.07 [s, C^3], 76.51 [d, J_{P-C} = 10.52 Hz, C^e], 75.37 [d, J_{P-C} = 7.98 Hz, C^d], 28.16 [s, C^b], 24.79 [s, C^c], 23.05 [s, C$^{c'}$]. ^{31}P NMR (162 MHz, $CDCl_3$): δ = 1.98 [s, J_{P-Pt} = 3851 Hz]. EI-MS: *m*/*z* 1576.3 [M]$^+$, 1540.4 [M − Cl]$^+$. Anal. found (calc. for $C_{72}H_{72}Cl_2FeN_2O_2P_2Pt_2$): C, 55.12 (54.86); H, 4.73 (4.60); N, 1.63 (1.78).

[Pt(CH$_3$){(OC$_6$H$_4$)CH═N{2,6-(Me$_2$CH)$_2$(C$_6$H$_3$)}}(PPh$_3$)] (6). To a methanol solution (10 ml) of imine **L$_A$** (0.206 g, 0.73 mmol), sodium acetate (0.06 g, 0.73 mmol) was added. The reaction mixture was allowed to stir at room temperature for 30 min. This mixture was slowly added to a methanol solution (10 ml) of [PtCl(cod)Me] (0.258 g, 0.73 mmol) at room temperature, giving a clear yellow mixture. PPh_3 (0.192 g, 0.73 mmol) was then added, resulting in the formation of a yellow precipitate. The reaction mixture was left to stir at room temperature for 16 h, after which it was filtered through Celite, and the solvent was removed *in vacuo* to give a light yellow solid. The crude product was dissolved in a minimum amount of CH_2Cl_2 and then passed through a SiO_2 column. Elution

with an *n*-hexane–ethyl acetate (95 : 5) solution produced a yellow band that was collected and concentrated to give **6**. Yield 0.472 g (86%). M.p.: 254–256 °C. IR (KBr): ν (CH=N) 1608 cm^{-1}. ^1H NMR (300 MHz, $CDCl_3$): δ = 8.11 [d, $^4J_{P-H}$ = 12.25 Hz, $^3J_{Pt-H}$ = 70.88 Hz, 1H, H^a], 7.73–7.67 (m, 6H, Ph–H), 7.44–7.33 (m, 9H, Ph–H), 7.27 [dt, $^3J_{H-H}$ = 8.62 Hz, $^3J_{H-H}$ = 1.81 Hz, 1H, H^4], 7.21–7.16 [m, ^3H, $H^{3',4',5'}$], 7.10 [dd, $^3J_{H-H}$ = 7.92 Hz, $^4J_{H-H}$ = 1.86 Hz, 1H, H^2], 6.45–6.42 [m, 2H, $H^{3,5}$], 3.59 [hept, 2H, H^b], 1.37 [d, $^3J_{H-H}$ = 6.87 Hz, 6H, $H^{c'}$], 1.14 [d, $^3J_{H-H}$ = 6.85 Hz, 6H, H^c], −0.29 [d, $^3J_{P-H}$ = 3.19 Hz, $^2J_{Pt-H}$ = 73.34 Hz, 3H, H^d]. ^{13}C NMR (101 MHz, $CDCl_3$): δ = 166.74 [s, $C^{1'}$], 162.12 [s, C^a], 146.76 [s, C^6], 141.54 [s, $C^{2',6'}$], 135.00 [s, C^2], 134.89 [Ph–C], 134.64 [s, C^4], 130.25 [d, J_{P-C} = 2.08 Hz, Ph–C], 129.73 [s, C^1], 127.75 [d, J_{P-C} = 10.80 Hz, Ph–C], 126.65 [s, $C^{4'}$], 123.15 [s, $C^{5,3',5'}$], 113.95 [s, C^3], 27.56 [s, C^b], 25.13 [s, C^c], 22.54 [s, $C^{c'}$], −18.93 [d, J_{P-C} = 8.97 Hz, C^d]. ^{31}P NMR (121 MHz, $CDCl_3$): δ = 20.43 [s, J_{P-Pt} = 4399.74 Hz]. EI-MS: *m*/*z* 753.3 $[M]^+$, 513.1 $[M - (O\text{-}Ph) - (2,6\text{-}^iPr\text{-}Ph)]^+$. Anal. found (calc. for $C_{31}H_{25}ClNOPPt$): C, 60.04 (60.63); H, 5.66 (5.36); N, 1.63 (1.86).

Isomerization kinetics (3a → 3b)

An NMR tube (5 mm) was charged with 15 mg of **3a**, which was then dissolved at room temperature (293 K) in chloroform-d to a fixed volume of 600 ± 5 μl. The tube was placed in the thermostated probe. The conversion **3a** → **3b** was then followed by conventional ^{31}P NMR spectroscopy. All reactions obeyed a first-order rate law until over 90% completion of the reaction. Relative concentration of **3a** *vs.* time data were acquired from the ^{31}P NMR signal areas of **3a** and **3b** and plotted as $\ln(a_0/a_t)$ *vs.* *t* (a_0 = relative concentration of **3a** before heating = 100%; a_t = relative concentration of **3a** at time, *t*) to obtain first-order rate constants k_{obs} from least-squares slopes (standard errors are also given). Activation parameters were derived from a linear least-squares analysis of $\ln(k_{obs}/T)$ *vs.* T^{-1} data according to the linear expression of the Eyring equation:[5]

$$\ln\frac{k}{T} = \frac{-\Delta H^{\ddagger}}{R} + \ln\frac{k_B}{h} + \frac{-\Delta S^{\ddagger}}{R} \quad (2)$$

(where R = 1.986 cal mol^{-1} K^{-1}, k_B = 8.62 × 10^{-5} eV K^{-1}, h = 4.14 × 10^{-15} eV S) and are listed in Table 5.

Computational methods

Hardware. The hardware used for the molecular modelling was the "Sun Hybrid System" based at the Centre of High Performance Computing (CHPC) in Cape Town, South Africa.

Software. All computational studies were performed using the DMol3 density functional theory (DFT) code[40] as implemented in Accelrys Materials Studio (Version 5.5). The nonlocal generalized gradient approximation (GGA) exchange-correlation functional was employed in all geometry optimizations, *viz.*, the PW91 functional of Perdew and Wang.[41] An all-electron polarized split valence basis set, termed double numeric polarized (DNP), was used. All geometry optimizations employed highly efficient delocalized internal coordinates.[42] The tolerance for convergence of the self-consistent field (SCF) density was set to 1 × 10^{-5} hartrees, while the tolerance for energy convergence was set to 1 × 10^{-6} hartrees. Additional convergence criteria include the tolerance for converged gradient (0.002 hartrees $Å^{-1}$) and the tolerance for converged atom displacement (0.005 Å). The thermal smearing option in Materials Studio makes use of a fractional electron occupancy scheme at the Fermi level according to a finite-temperature Fermi function.[41,43]

In all cases optimized geometries were subjected to full frequency analyses at the same GGA/PW91/DNP level of theory to verify the nature of the stationary points. Equilibrium geometries were characterized by the absence of imaginary frequencies. Preliminary transition state geometries were obtained by either the DMol3 PES scan functionality in Cerius[44] (Version 5.5, Accelrys, Inc.) or the integrated linear synchronous transit/quadratic synchronous transit (LST/QST) algorithm[45] available in Materials Studio. These preliminary structures were then subjected to full TS optimizations using an eigenvector-following algorithm. All transition structure geometries exhibited only one imaginary frequency in the reaction coordinate.

All calculations were performed without the incorporation of solvent effects. All results were mass balanced for the isolated system in the gas phase. The reported energies refer to Gibbs free energy at 298.15 K and 1 atm.

Acknowledgements

Acknowledgements go to the National Research Foundation (South Africa) and the DST/NRF COE in Catalysis (c*change) for funding. This work was also supported by Research Committees of the University of Cape Town and Stellenbosch University. The authors wish to acknowledge Centre for High Performance Computing (CHPC) in Cape Town, South Africa for computational resources as well.

References

1 N. E. A. El-Gamel, *RSC Adv.*, 2012, **2**, 5870.
2 (*a*) C. Wang, S. Friedrich, T. R. Younkin, R. T. Li, R. H. Grubbs, D. A. Bansleben and M. W. Day, *Organometallics*, 1998, **17**, 3149; (*b*) T. R. Younkin, E. F. Connor, J. I. Henderson, S. Friedrich, R. H. Grubbs and D. A. Bansleben, *Science*, 2000, **287**, 460; (*c*) X. F. Li and Y. S. Li, *J. Polym. Sci., Part A: Polym. Chem.*, 2002, **40**, 2680.
3 (*a*) Y. Liu, M. G. B. Drew and Y. Liu, *J. Mol. Struct. (THEOCHEM)*, 2007, **809**, 29; (*b*) J. Cui, M. Zhang and Y. Zhang, *Inorg. Chem. Commun.*, 2010, **13**, 81.
4 (*a*) P. Chellan, T. Stringer, A. Shokar, P. J. Dornbush, G. Vazquez-Anaya, K. M. Land, K. Chibale and G. S. Smith, *J. Inorg. Biochem.*, 2011, **105**, 1562; (*b*) P. Chellan, N. Shunmoogam-Gounden, D. T. Hendricks, J. Gut, P. J. Rosenthal, C. Lategan, P. J. Smith, K. Chibale and G. S. Smith, *Eur. J. Inorg. Chem.*, 2010, **22**, 3520;

(*c*) W. Henderson, C. Evans, B. K. Nicholson and J. Fawcett, *Dalton Trans.*, 2003, 2691.

5 (*a*) N. Komiya, T. Muraoka, M. Iida, M. Miyanaga, K. Takahashi and T. Naota, *J. Am. Chem. Soc.*, 2011, **133**, 16054; (*b*) N. Komiya, M. Okada, K. Fukumoto, D. Jomori and T. Naota, *J. Am. Chem. Soc.*, 2011, **133**, 6493; (*c*) C.-M. Che, C.-C. Kwok, S.-W. Lai, A. F. Rausch, W. J. Finkenzeller, N. Zhu and H. Yersin, *Chem.–Eur. J.*, 2010, **16**, 233.

6 Y. Suzuki, H. Terao and T. Fujita, *Bull. Chem. Soc. Jpn.*, 2003, **76**, 1493.

7 D. J. Jones, V. C. Gibson, S. M. Green, P. J. Maddox, A. White and D. J. Williams, *J. Am. Chem. Soc.*, 2005, **127**, 11037.

8 (*a*) M. S. W. Chan, L. Deng and T. Ziegler, *Organometallics*, 2000, **19**, 2741; (*b*) T. R. Younkin, R. H. Grubbs, L. M. Henling and M. W. Day, *Abstr. Pap. Am. Chem. Soc.*, 2001, **221**, INOR-253; (*c*) Y. Liu, M. G. B. Drew and Y. Liu, *J. Mol. Struct. (THEOCHEM)*, 2007, **821**, 30.

9 (*a*) W. Heyndrickx, G. Occhipinti, Y. Minenkov and V. R. Jensen, *Chem.–Eur. J.*, 2011, **17**, 14628; (*b*) D. V. Deubel and T. Ziegler, *Organometallics*, 2002, **21**, 4432.

10 I. Kenichi, W. Akira and K. Kaoru, *Jpn. Kokai Tokyo Koho*, JP 2001072654 (A), 2001.

11 J. Cui, M. Zhang and Y. Zhang, *Inorg. Chem. Commun.*, 2010, **13**, 81.

12 M. Crespo, R. Martin, T. Calvet, M. Font-Bardia and X. Solans, *Polyhedron*, 2008, **27**, 2603.

13 P. Bhattacharyya, J. Parr and A. M. Z. Slawin, *J. Chem. Soc., Dalton Trans.*, 1998, 3609.

14 (*a*) J. Forniés, V. Sicilia, C. Larraz, J. A. Camerano, A. Martín, J. M. Casas and A. C. Tsipis, *Organometallics*, 2010, **29**, 1396; (*b*) P. D. Smith, T. Gelbrich and M. B. Hursthouse, *J. Organomet. Chem.*, 2002, **659**, 1; (*c*) C. A. Craig, F. O. Garces, R. J. Watts, R. Palmans and A. J. Frank, *Coord. Chem. Rev.*, 1990, **97**, 193; (*d*) M. M. Mdleleni, J. S. Bridgewater, R. J. Watts and P. C. Ford, *Inorg. Chem.*, 1995, **34**, 2334; (*e*) A. Zucca, G. L. Petretto, S. Stoccoro, M. A. Cinellu, M. Manassero, C. Manassero and G. Minghetti, *Organometallics*, 2009, **28**, 215.

15 P. S. Pregosin and R. W. Kunz, in *^{31}P and ^{13}C NMR of Transition Metal Phosphine Complexes*, ed. in P. Diehl, E. Fluck and R. Kosfeld, Springer-Verlag, Berlin, 1979.

16 O. M. Ní Dhubhghaill, J. Lennona and M. G. B. Drew, *Dalton Trans.*, 2005, 3213.

17 R. Munzenberg, P. Rademacher and R. Boese, *J. Mol. Struct.*, 1998, **444**, 77.

18 Y. Murata, H. Ohgi, T. Fujihara, J. Terao and Y. Tsuji, *Inorg. Chim. Acta*, 2011, **368**, 237.

19 J.-F. Ma and Y. Yamamoto, *Inorg. Chim. Acta*, 2000, **299**, 164.

20 The sum of the internal angles of planar six-membered ring is 720°.

21 W. S. Knowles, B. D. Vineyard, M. J. Sabacky, G. L. Bachmann and D. J. Weinkauff, *J. Am. Chem. Soc.*, 1977, **99**, 5946.

22 R. Martín, M. Crespo, M. Font-Bardia and T. Calvet, *Polyhedron*, 2009, **28**, 1369.

23 (*a*) S. S. Zumdahl and R. S. Drago, *J. Am. Chem. Soc.*, 1968, **90**, 6669; (*b*) W. L. Steffen and G. J. Palenik, *Inorg. Chem.*, 1976, **15**, 2432.

24 T. G. Appleton and M. A. Bennett, *Inorg. Chem.*, 1978, **17**, 738.

25 A. Capapé, M. Crespo, J. Granell, M. Font-Bardía and X. Solans, *J. Organomet. Chem.*, 2005, **690**, 4309.

26 H. Makio, N. Kashiwa and T. Fujita, *Adv. Synth. Catal.*, 2002, **344**, 477.

27 (*a*) E. Guido, G. D'Amico, N. Russo, E. Sicilia, S. Rizzato, A. Albinati, A. Romeo, M. R. Plutino and R. Romeo, *Inorg. Chem.*, 2011, **50**, 2224; (*b*) A. L. Casado and P. Espinet, *Organometallics*, 1998, **17**, 954.

28 (*a*) R. G. Wilkins, *Kinetics and Mechanism of Reactions of Transitions Metal Complexes*, VCH, Weinheim, 2nd edn, 1991; (*b*) G. Alibrandi, L. M. Scolaro and R. Romeo, *Inorg. Chem.*, 1991, **30**, 4007 and references therein; (*c*) U. Frey, L. Helm, A. E. Merbach and R. Romeo, *J. Am. Chem. Soc.*, 1989, **111**, 8161.

29 L. J. Goossen, D. Koley, H. L. Hermann and W. Thiel, *Organometallics*, 2005, **24**, 2398.

30 F. Basolo and G. Pearson, *Mechanism of Inorganic Reactions*, Wiley, New York, 2nd edn, 1967.

31 (*a*) G. K. Anderson and R. J. Cross, *Chem. Soc. Rev.*, 1980, **9**, 185; (*b*) R. S. Berry, *J. Chem. Phys.*, 1960, **32**, 933.

32 (*a*) F. Ozawa, T. Ito, Y. Nakamura and A. Yamamoto, *Bull. Chem. Soc. Jpn.*, 1981, **54**, 1868; (*b*) R. S. Pavonessa and W. C. Trogler, *J. Am. Chem. Soc.*, 1982, **104**, 3529.

33 (*a*) J. J. Low and W. A. Goddard III, *J. Am. Chem. Soc.*, 1986, **108**, 6115; (*b*) K. Tatsumi, R. Hoffmann, A. Yamamoto and J. K. Stille, *Bull. Chem. Soc. Jpn.*, 1981, **54**, 1857; (*c*) S. Noda, A. Nakamura, T. Kochi, L. W. Chung, K. Morokuma and K. Nozaki, *J. Am. Chem. Soc.*, 2009, **131**, 14088.

34 S. Sakaki, N. Mizoe, Y. Musashi and M. Sugimoto, *J. Mol. Struct. (THEOCHEM)*, 1999, **461–462**, 533.

35 Z. Otwinowski and W. Minor, *Methods in Enzymology, Macromolecular Crystallography*, ed. C. W. Carter Jr and R. M. Sweet, Academic Press, part A, 1997, vol. 276, pp. 307–326.

36 G. M. Sheldrick, *SADABS*, University of Göttingen, Germany, 1996.

37 G. M. Sheldrick, *SHELXL-97 and SHELXS-97*, University of Göttingen, Germany, 1997.

38 L. J. Barbour, *J. Supramol. Chem.*, 2001, **1**, 189.

39 (*a*) J. H. Price, A. N. Williamson, R. F. Schramm and B. B. Wayland, *Inorg. Chem.*, 1972, **11**, 1280; (*b*) V. Y. Kukushkin, A. J. L. Pombeiro, C. M. P. Ferreira and L. I. Elding, *Inorg. Synth.*, 2002, **33**, 189.

40 (*a*) B. Delley, *J. Chem. Phys.*, 1992, **92**, 508; (*b*) B. Delley, *J. Phys. Chem.*, 1996, **100**, 6107; (*c*) B. Delley, *J. Chem. Phys.*, 2000, **113**, 7756.
41 J. P. Perdew and Y. Wang, *Phys. Rev. B: Condens. Matter*, 1992, **45**, 13244.
42 J. Andzelm, R. D. King-Smith and G. Fitzgerald, *Chem. Phys. Lett.*, 2001, **335**, 321.
43 M. Weinert and J. W. Davenport, *Phys. Rev. B: Condens. Matter*, 1992, **45**, 13709.
44 D. Vogt, in *Applied Homogeneous Catalysis with Organometallic Compounds*, ed. B. Cornils and W. A. Herrmann, VCH, Weinheim, Germany, 1996, p. 245.
45 N. Govind, M. Petersen, G. Fitzgerald, D. King-Smith and J. Andzelm, *Comput. Mater. Sci.*, 2003, **28**, 250.